NuInt 17

26/06/2017

NEW

ν_μ inclusive CC cross-section measurement on C at T2K

Alfonso Garcia and Federico Sanchez

for the T2K collaboration

Inclusive Cross Section:

- Inclusive measurements are valuable:
    - High purity and efficiency.
    - Hadron information is almost not used.
    - Test different channel predictions from models.

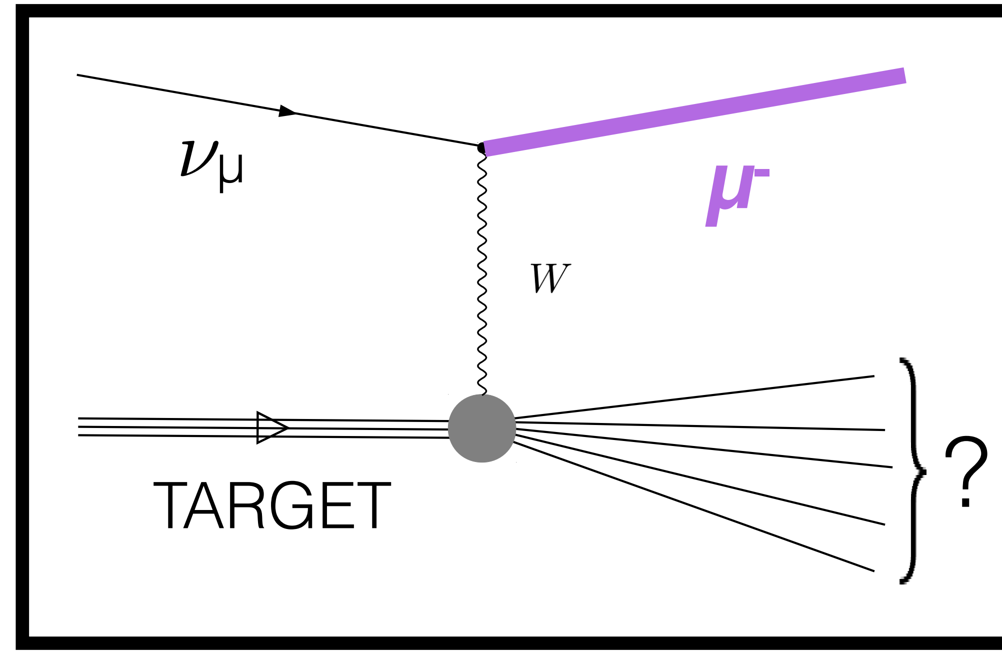

- T2K already published a ν_μ CC inclusive cross section using the off-axis near detector in 2013 (PRD87).
    - Statistics was limited → loose binning.
    - Simple event selection → phase space restricted to forward region of the outgoing μ^-.

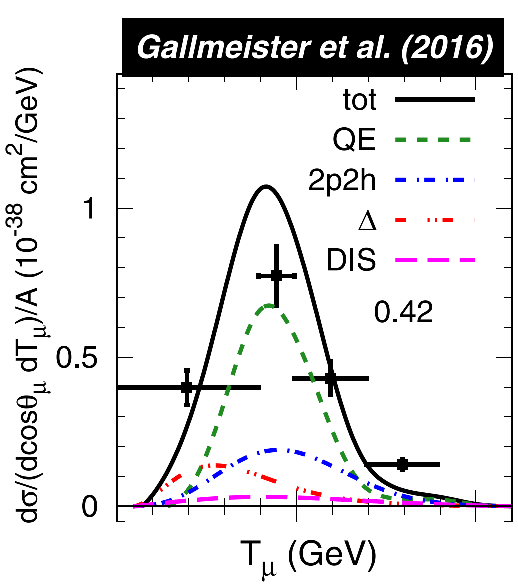

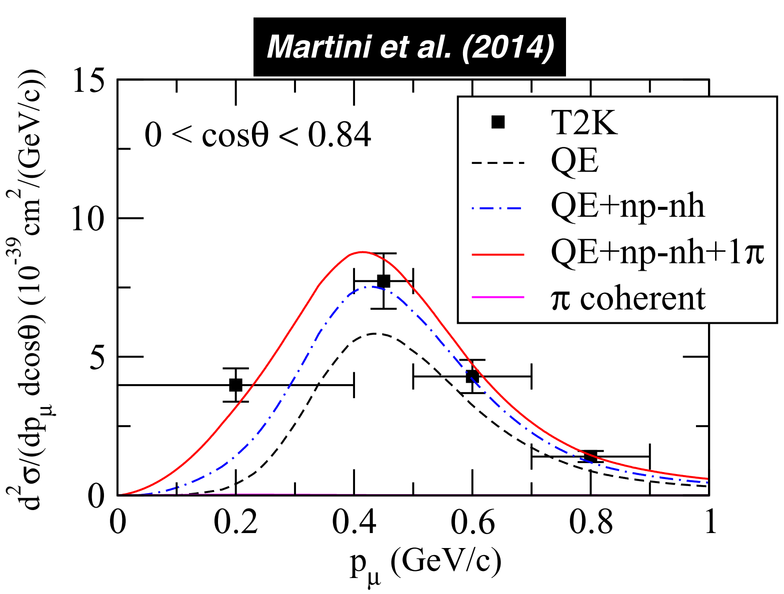

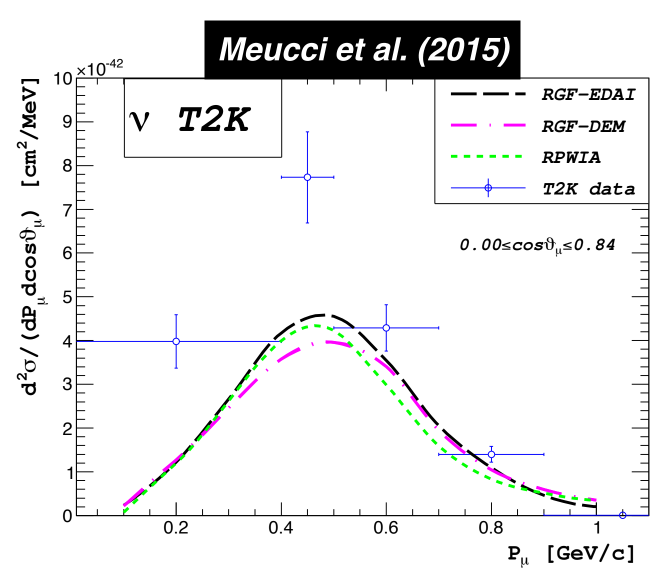

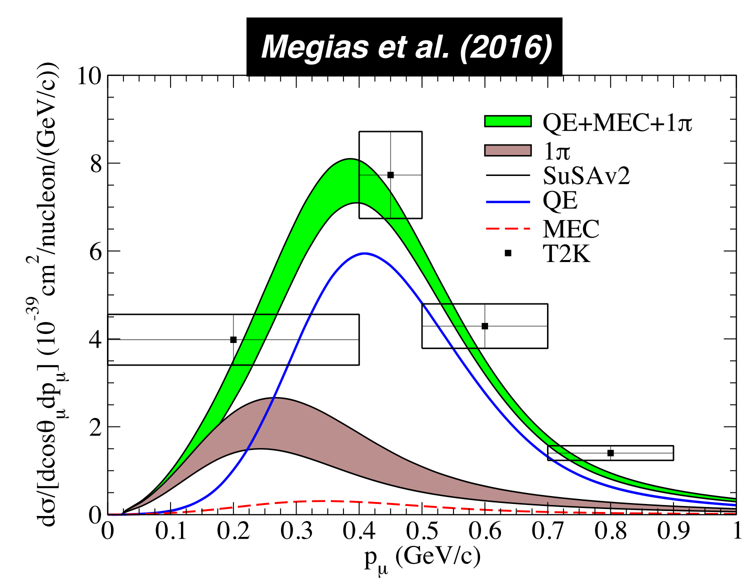

NEW

Off-Axis Inclusive Cross Section:

Goal -> double-differential (p_μ,$\cos\theta_\mu$) cross section ν_μ CC inclusive on plastic*

*C[86%]H[7%]O[4%]

- Statistics has been increased by a factor of five.
- New event selection has been developed:
  - Increase the angular acceptance for high-angle and backward-going muons.
  - Reduce the pion contamination (main background).
- Full use of the off-axis near detector (ND280) is required.

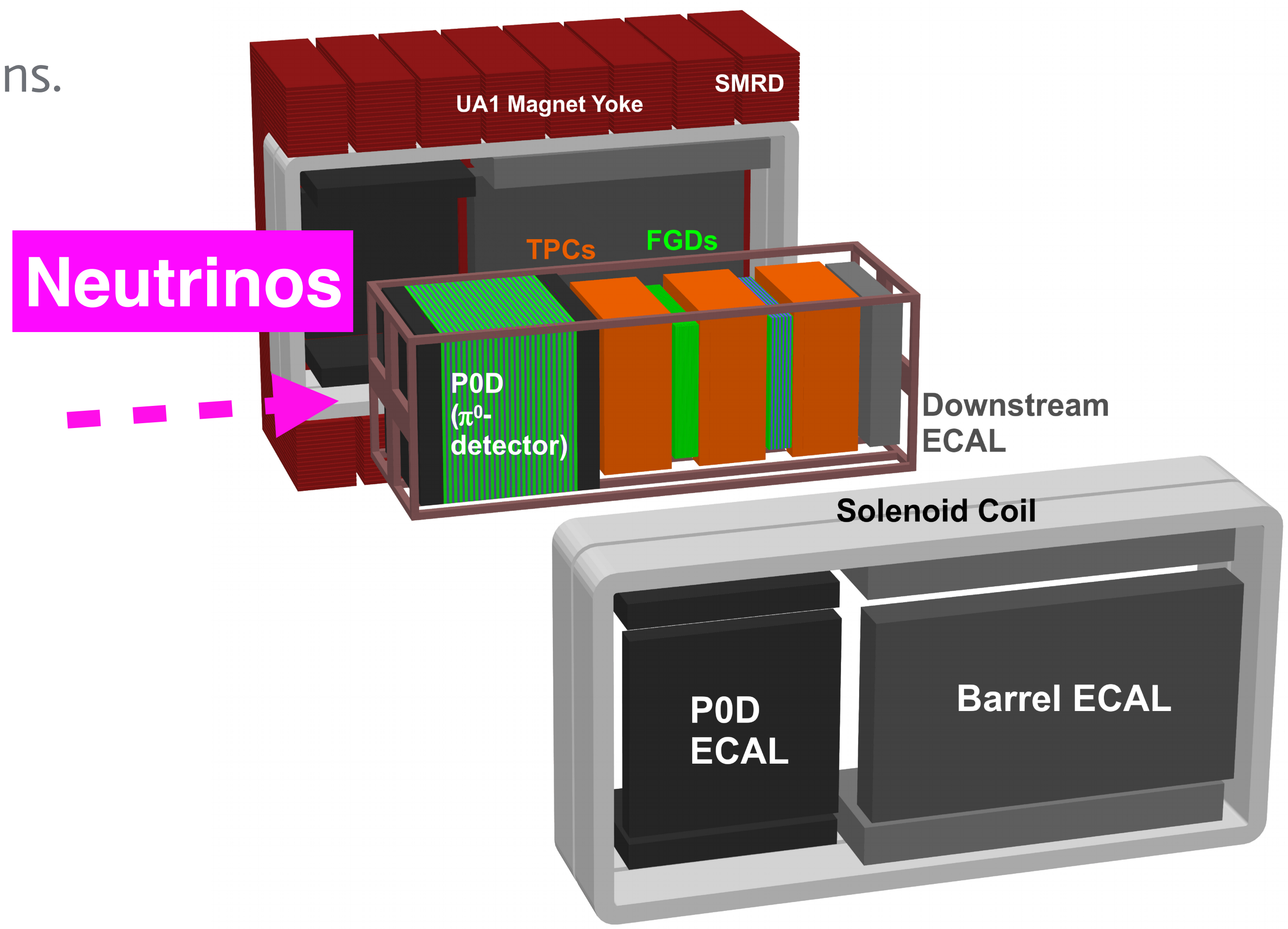

Previous ν_μ CC Selection:

- Event selection focused on the TRACKER region (FGDs+TPCs).
  - Select tracks starting in the FGD1 entering in TPC2.

Two FGDs
(Fine Grained Detector)
[plastic scintillators layers]

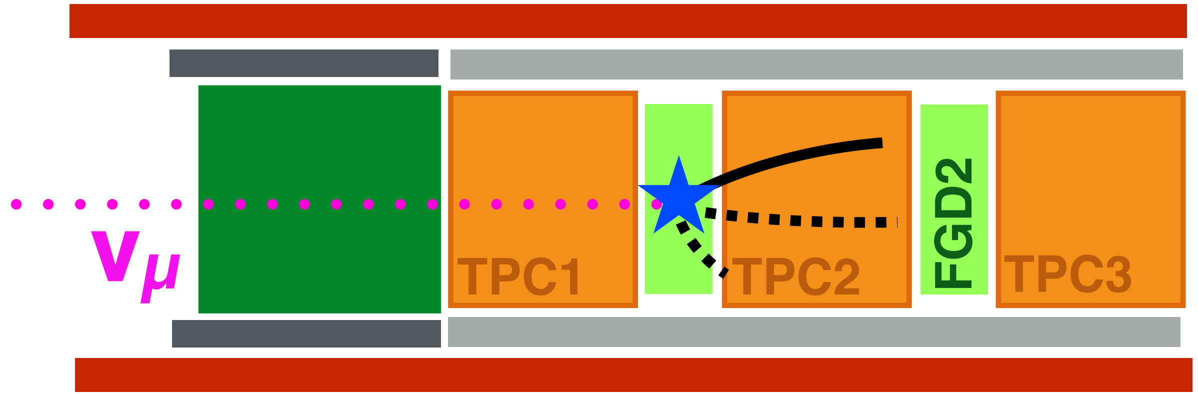

Previous ν_μ CC Selection:

- Event selection focused on the TRACKER region (FGDs+TPCs).
    - Select tracks starting in the FGD1 entering in TPC2.
    - Momentum/charge (curvature) and PID (energy loss) reconstructed using TPC.

Two FGDs
(Fine Grained Detector)
[plastic scintillators layers]

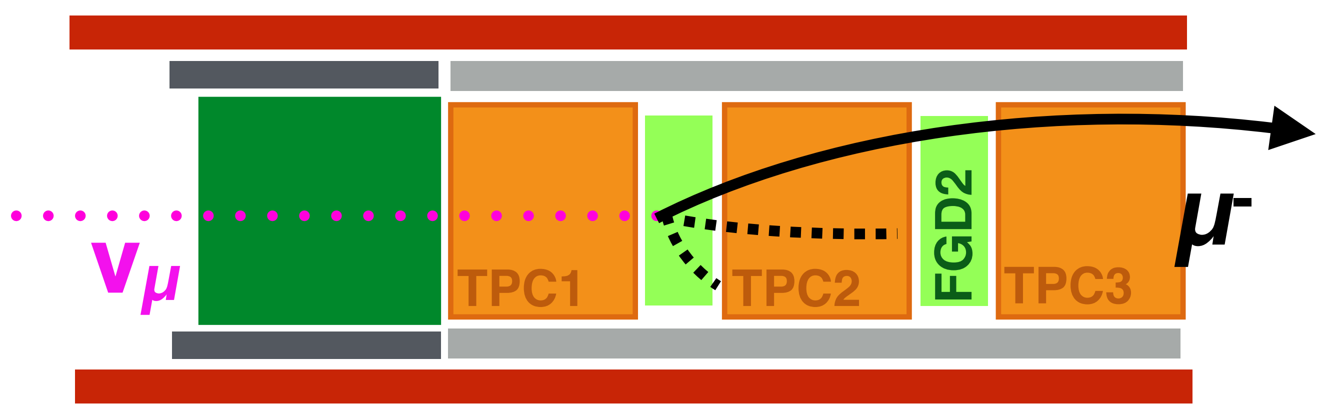

Three TPCs
(Time Projection Chamber)
[$Ar:CF_4:iC_4H_{10}$ [95:3:2]]

Previous ν_μ CC Selection:

- Event selection focused on the TRACKER region (FGDs+TPCs).
    - Select tracks starting in the FGD1 entering in TPC2.
    - Momentum/charge (curvature) and PID (energy loss) reconstructed using TPC.
    - Other detectors used as veto.

SMRD
(Side Muon Range Detector)
[plastic scintillator inside magnet yokes]

Two FGDs
(Fine Grained Detector)
[plastic scintillators layers]

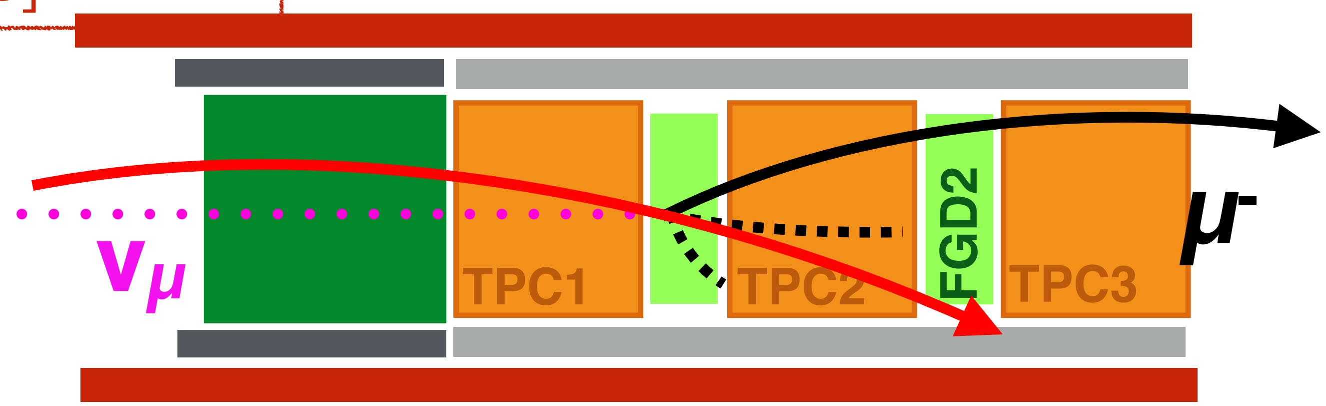

P0D
(π^0 detector)
[plastic scintillator modules interleaved with water, brass and lead layers]

ECal
(Electromagentic CALorimiter)
[plastic scintillator layers interleaved with lead]

Three TPCs
(Time Projection Chamber)
[$Ar:CF_4:iC_4H_{10}$ [95:3:2]]

NEW

ν_μ CC Selection:

- New ν_μ CC selection aims for full coverage in ND280.

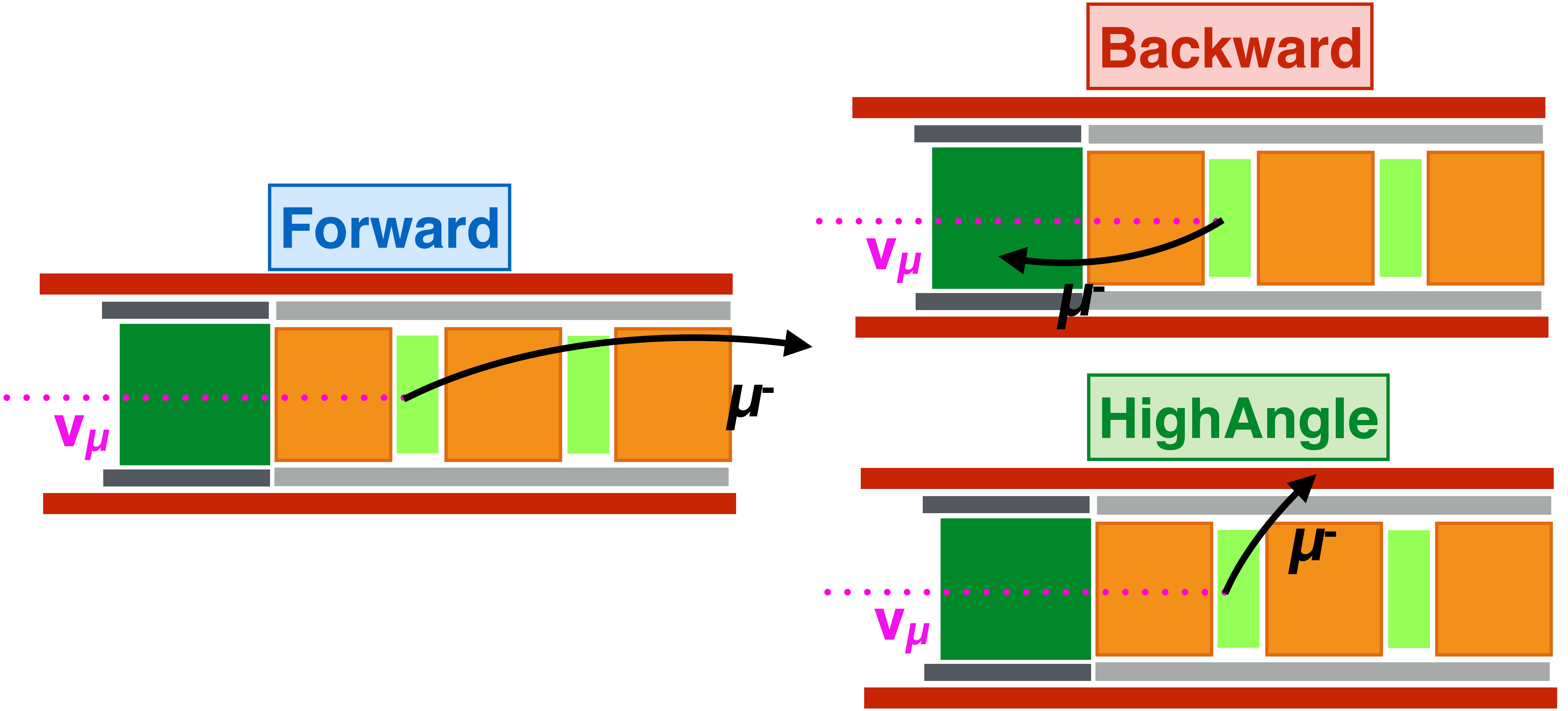

NEW

ν_μ CC Selection:

- New ν_μ CC selection aims for full coverage in ND280.
  - Select backward-going muons using timing (FGD1-FGD2 // FGD1-PoD // FGD1-ECAL).

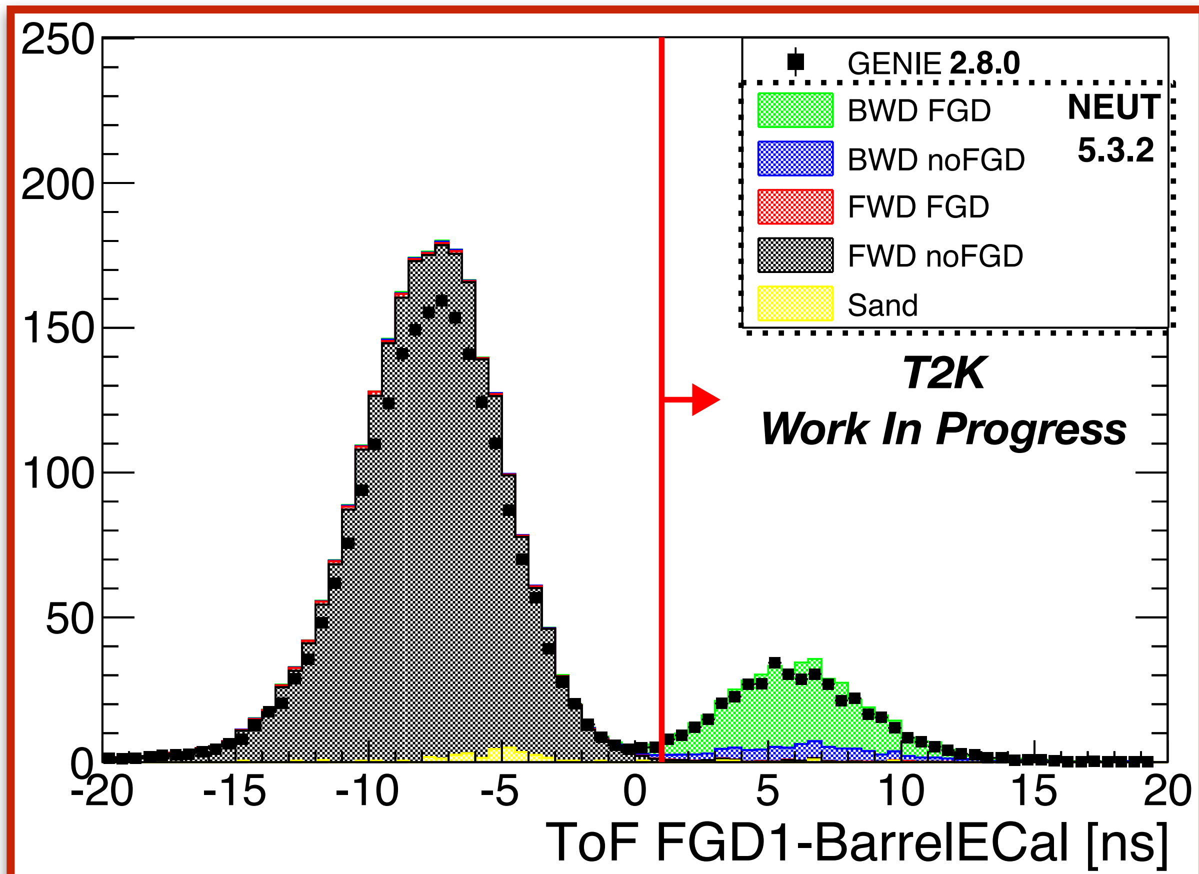

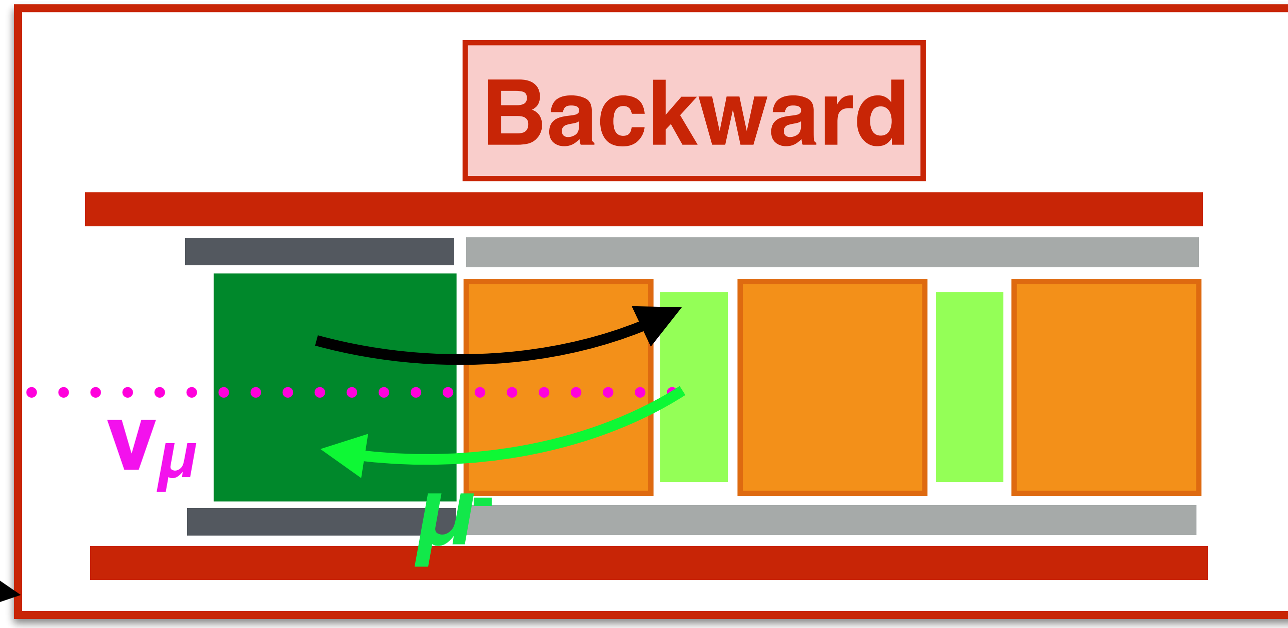

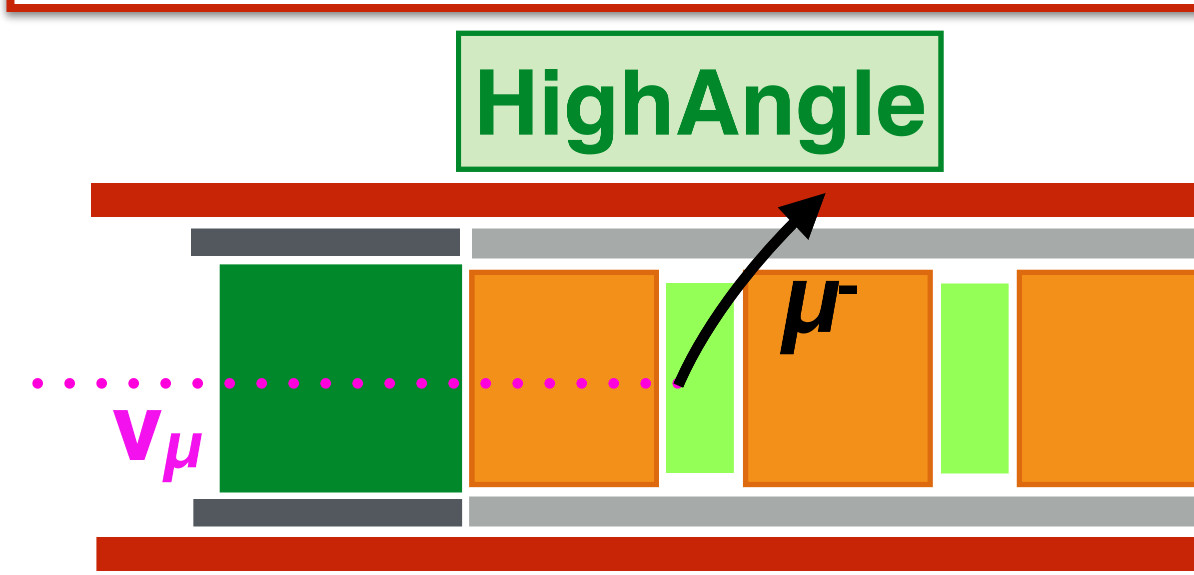

Timing from sub-detectors

NEW

ν_μ CC Selection:

- New ν_μ CC selection aims for full coverage in ND280.
  - Select backward-going muons using timing (FGD1-FGD2 // FGD1-PoD // FGD1-ECAL).
  - Select high-angle muons using calorimeter information.

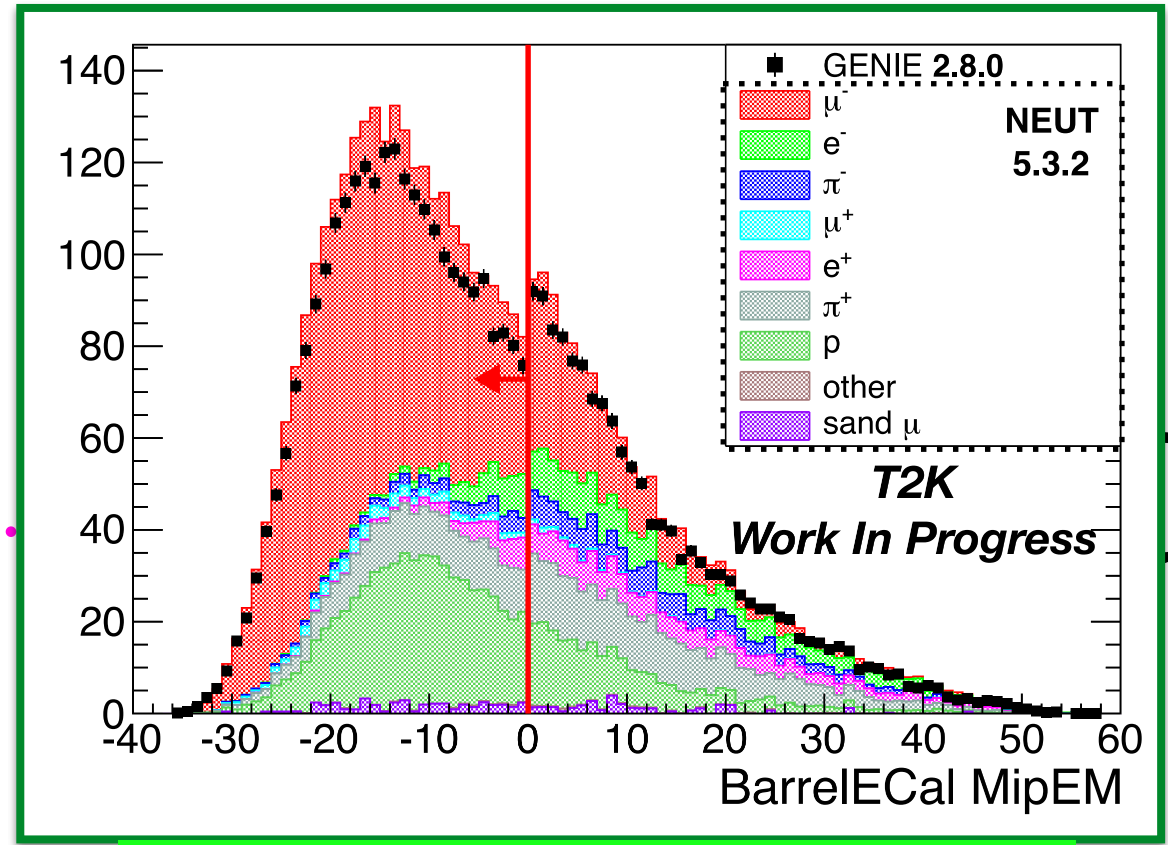

No TPC -> ECAL PID

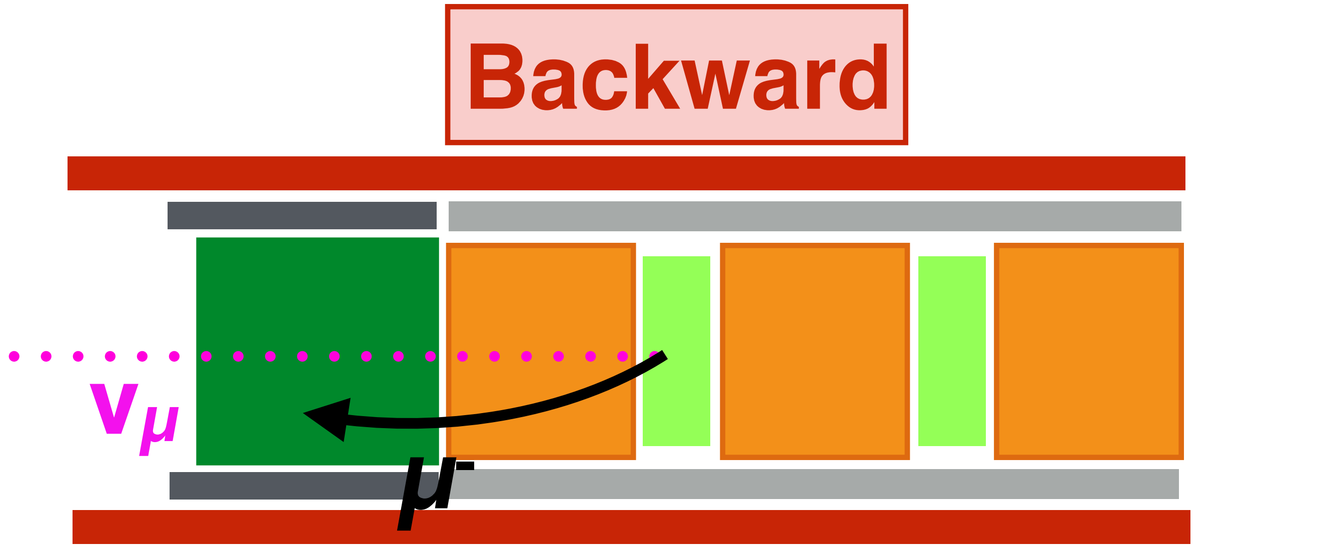

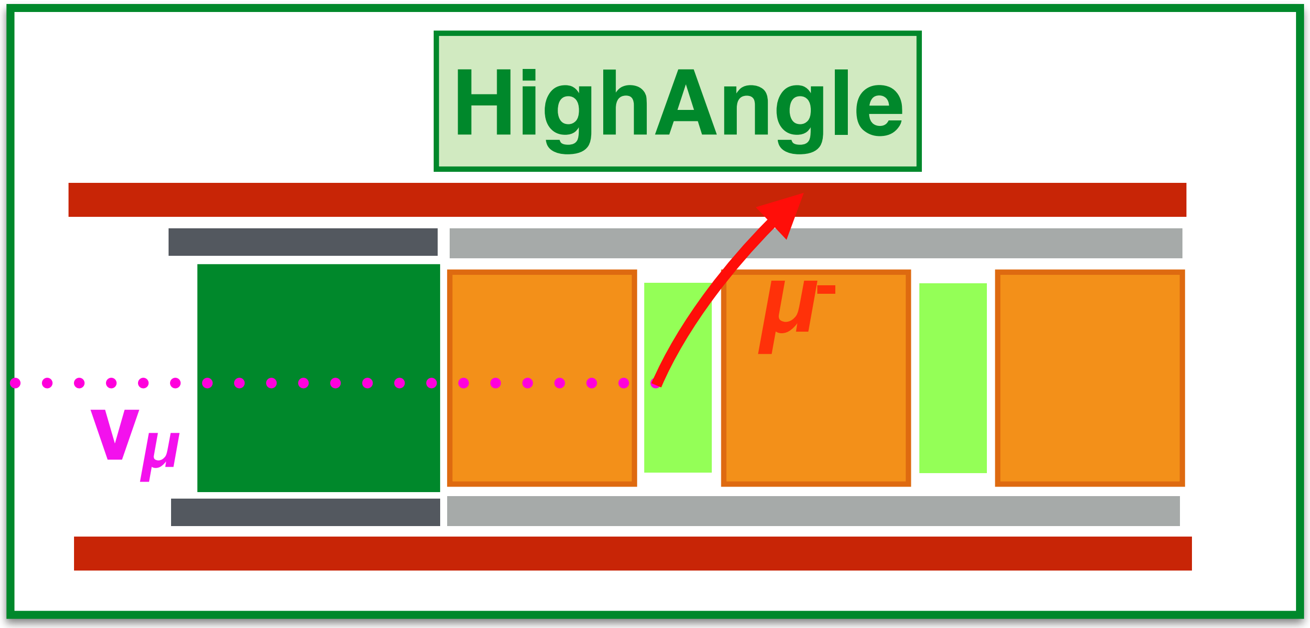

NEW

ν_μ CC Selection:

Clear improvement of angular acceptance & high purities

Forward -> FWD
Backward -> BWD
High-Angle Forward -> HAFWD
High-Angle Backward -> HABWD

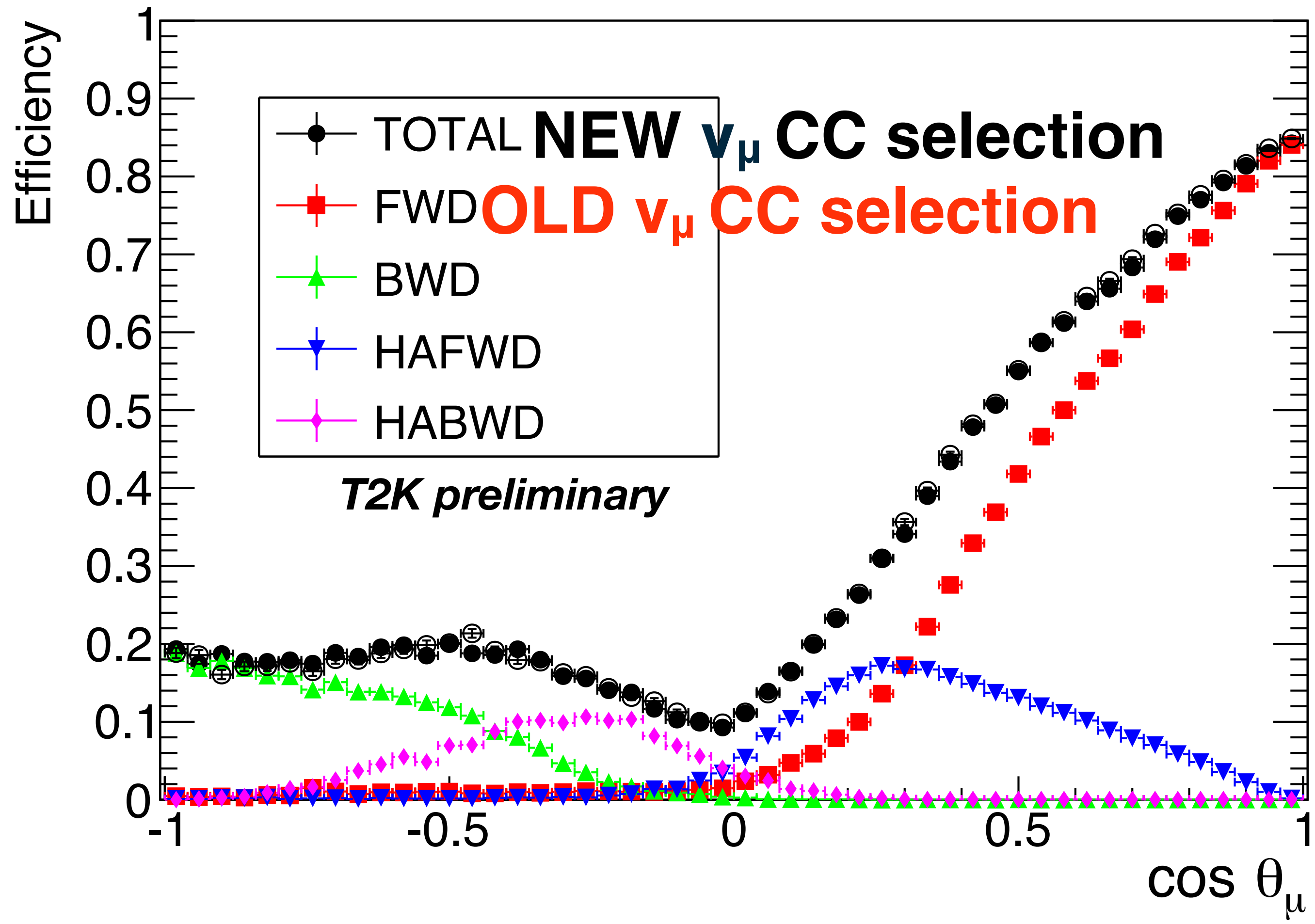

Purities	FWD	BWD	HAFWD	HABWD
ν_μ CC	89%	73%	82%	79%
$\bar{\nu}_\mu$ / ν_e / $\bar{\nu}_e$ CC or NC	6%	2%	6%	3%
Out of FV	4%	22%	11%	17%
Sand μ	1%	2%	1%	1%

Cross-section Extraction:

Goal -> double-differential (p_μ,$\cos\theta_\mu$) cross section ν_μ CC inclusive on plastic*

*C[86%]H[7%]O[4%]

$$\frac{d\sigma}{dp_{\mu,i}dcos\theta_{\mu,j}} = \frac{N_{ij}^{CC-\mu}}{\epsilon_{ij}^{CC-\mu,MC}\Phi N_{nucleons}^{FV}\Delta p_{\mu,i}\Delta cos\theta_{\mu,j}}$$

Cross-section Extraction:

Goal -> double-differential (p_μ,$\cos\theta_\mu$) cross section ν_μ CC inclusive on plastic*

*C[86%]H[7%]O[4%]

$$\frac{d\sigma}{dp_{\mu,i}dcos\theta_{\mu,j}} = \frac{N_{ij}^{CC-\mu}}{\epsilon_{ij}^{CC-\mu,MC}\Phi N_{nucleons}^{FV}\Delta p_{\mu,i}\Delta cos\theta_{\mu,j}}$$

- Flux integrated result:
  - Detector dependent.
  - Less model bias.

Cross-section Extraction:

Goal -> double-differential (p_μ,$\cos\theta_\mu$) cross section ν_μ CC inclusive on plastic*

*C[86%]H[7%]O[4%]

$$\frac{d\sigma}{dp_{\mu,i}dcos\theta_{\mu,j}} = \frac{N_{ij}^{CC-\mu}}{\epsilon_{ij}^{CC-\mu,MC}\Phi N_{nucleons}^{FV}\Delta p_{\mu,i}\Delta cos\theta_{\mu,j}}$$

- μ kinematics unfolded using maximum likelihood fit (PRD 93, 112012 [2016]).
- Background subtraction controlled with π- sidebands.

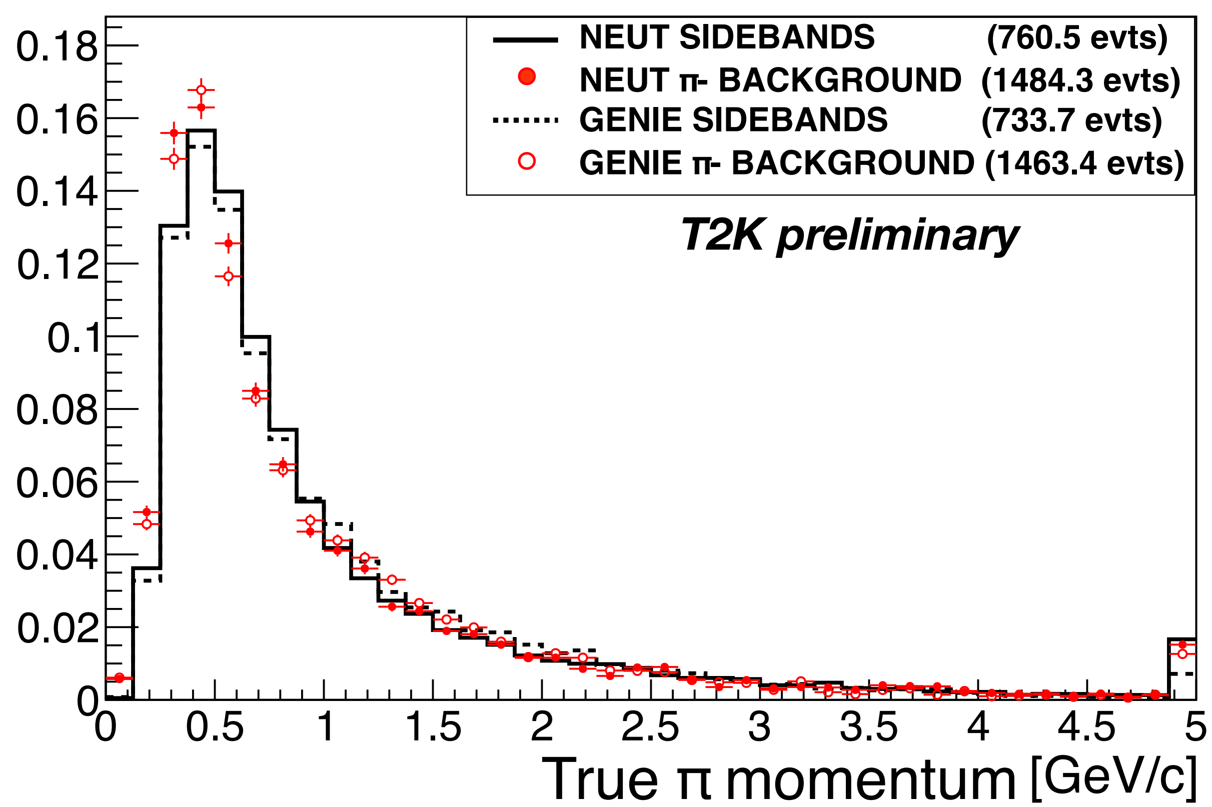

Cross-section Extraction:

Goal -> double-differential (p_μ,$\cos\theta_\mu$) cross section ν_μ CC inclusive on plastic*

*C[86%]H[7%]O[4%]

$$\frac{d\sigma}{dp_{\mu,i}dcos\theta_{\mu,j}} = \frac{N_{ij}^{CC-\mu}}{\epsilon_{ij}^{CC-\mu,MC}\Phi N_{nucleons}^{FV}\Delta p_{\mu,i}\Delta cos\theta_{\mu,j}}$$

- Efficiency correction using two different predictions.

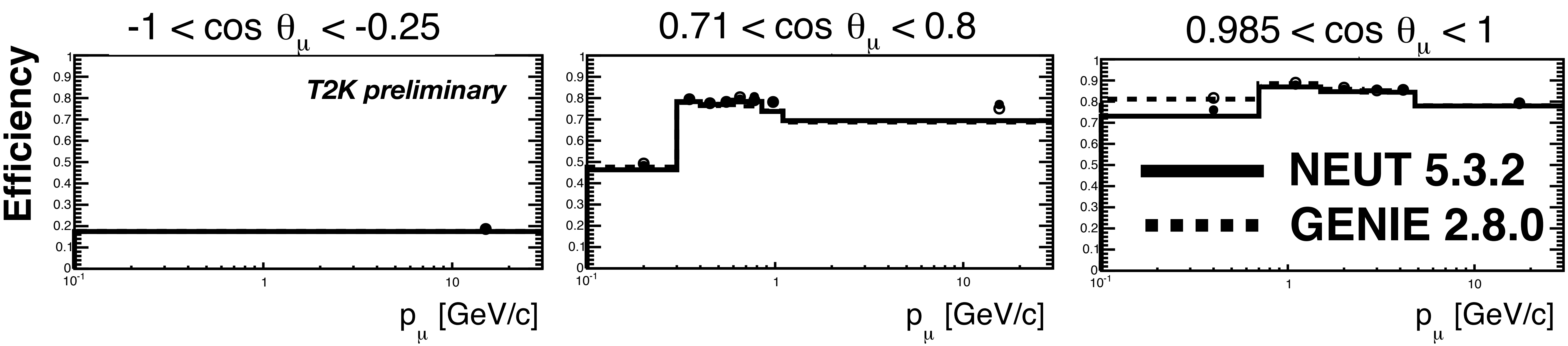

Cross-section Extraction:

Goal -> double-differential (p_μ,$\cos\theta_\mu$) cross section ν_μ CC inclusive on plastic*

*C[86%]H[7%]O[4%]

$$\frac{d\sigma}{dp_{\mu,i}dcos\theta_{\mu,j}} = \frac{N_{ij}^{CC-\mu}}{\epsilon_{ij}^{CC-\mu,MC}\Phi N^{FV}_{nucleons}\Delta p_{\mu,i}\Delta cos\theta_{\mu,j}}$$

- Efficiency correction using NEUT 5.3.0 and GENIE 2.8.0 predictions.
    - Discrepancies for low momentum muons going forward (in RES and DIS channels).

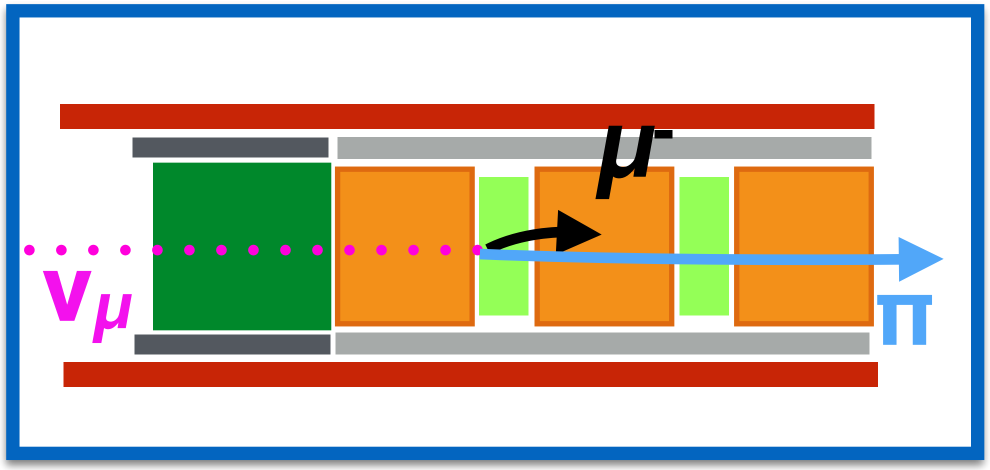

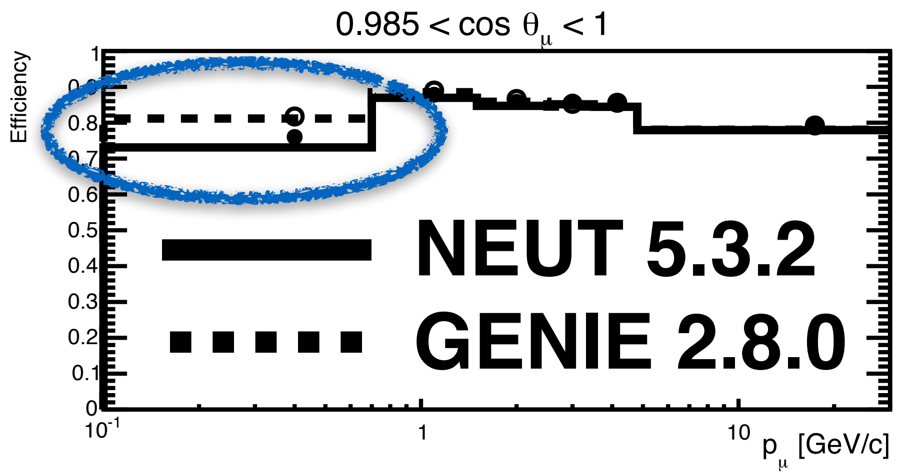

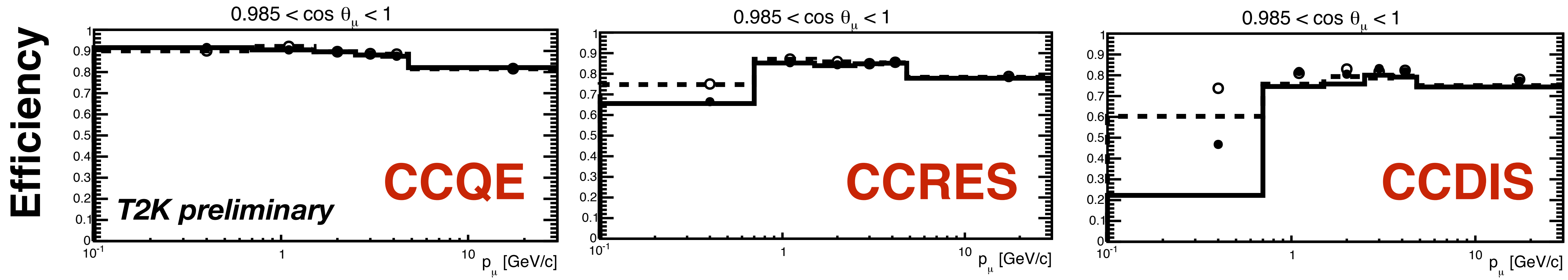

Cross-section Extraction:

Goal -> double-differential (p_μ,$\cos\theta_\mu$) cross section ν_μ CC inclusive on plastic*

$$\frac{d\sigma}{dp_{\mu,i}dcos\theta_{\mu,j}} = \frac{N_{ij}^{CC-\mu}}{\epsilon_{ij}^{CC-\mu,MC}\Phi N_{nucleons}^{FV}\Delta p_{\mu,i}\Delta cos\theta_{\mu,j}}$$

*C[86%]H[7%]O[4%]

~9% ~0.7%

- Source of errors →

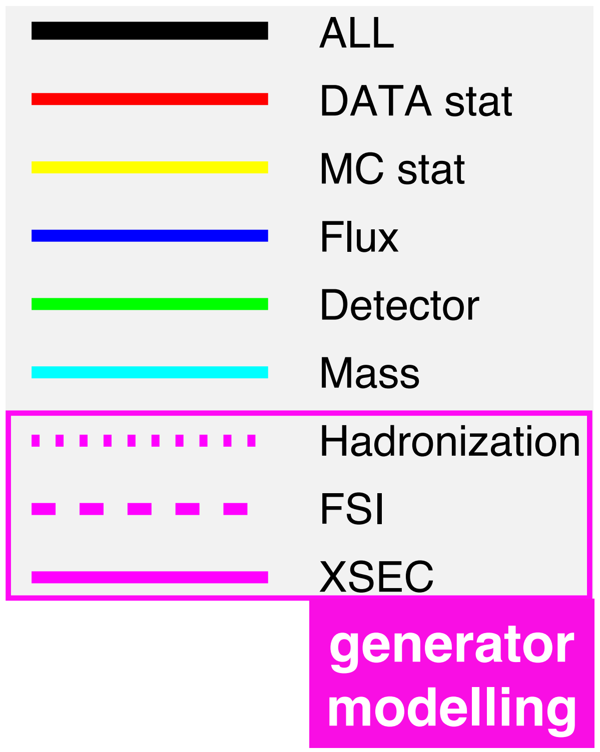

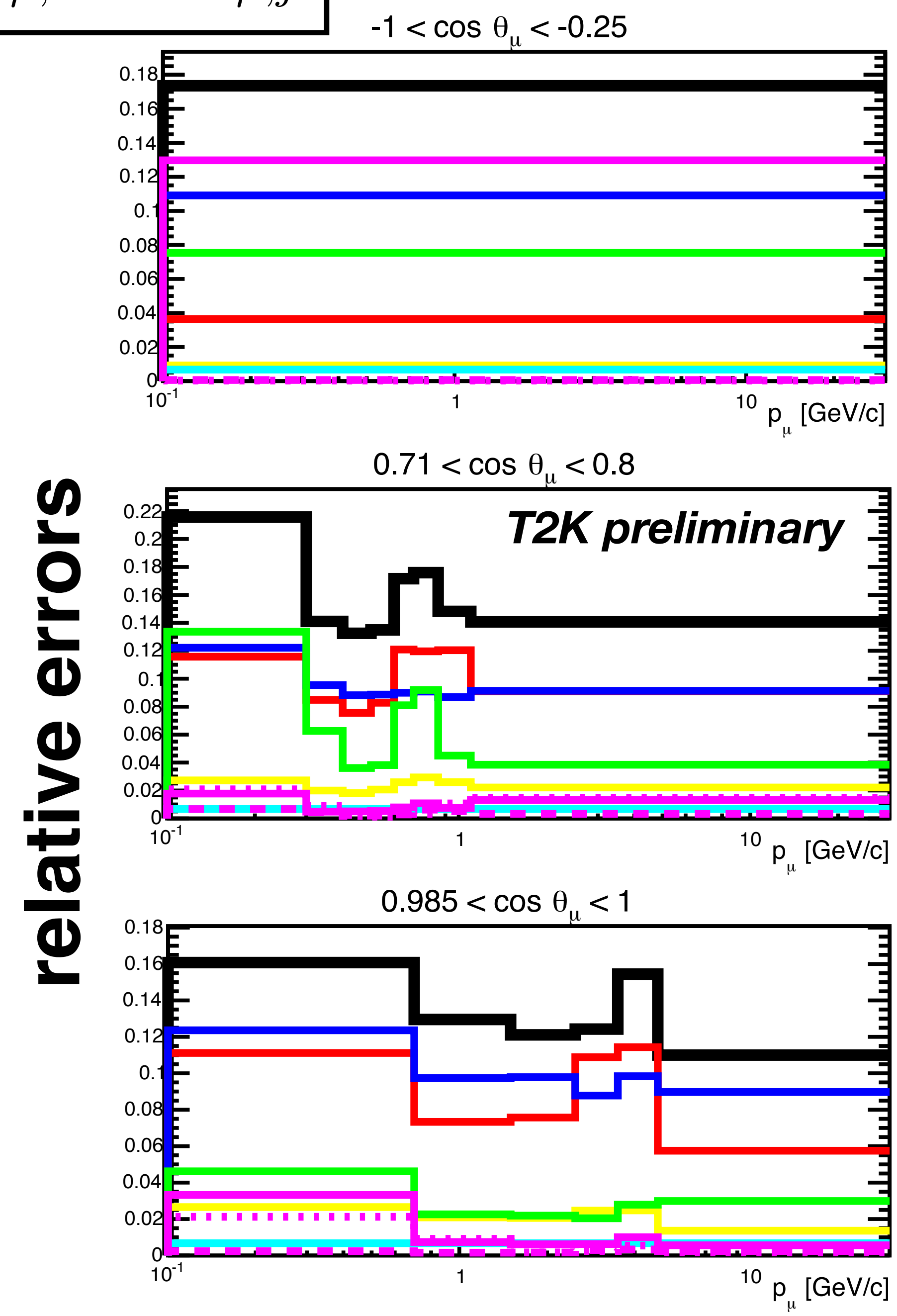

- Flux normalization uncertainty dominates, and generator modeling uncertainty is low (except backward region).

NEW

Results:

- Robust cross-section measurement (same results with two models).

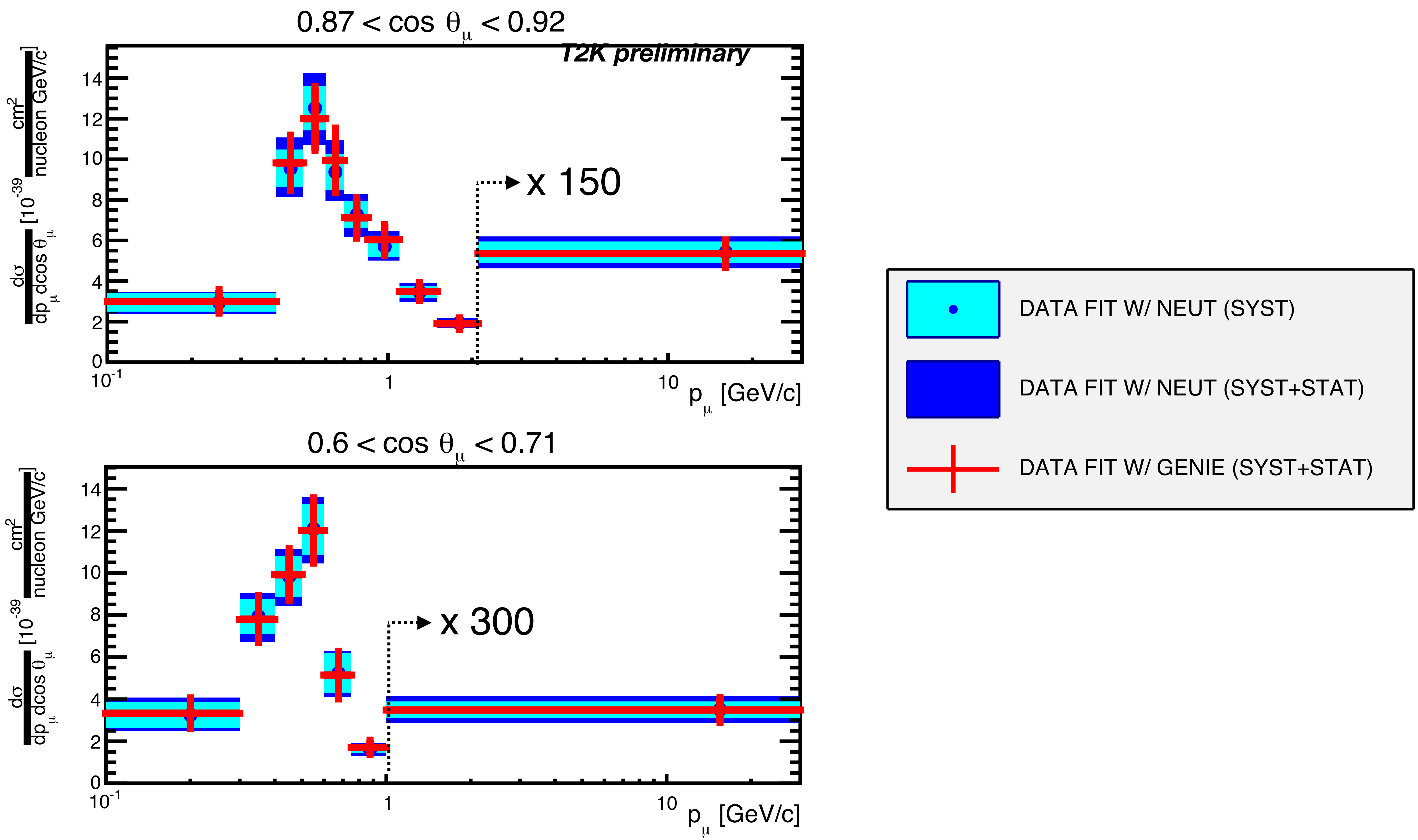

NEW Results:

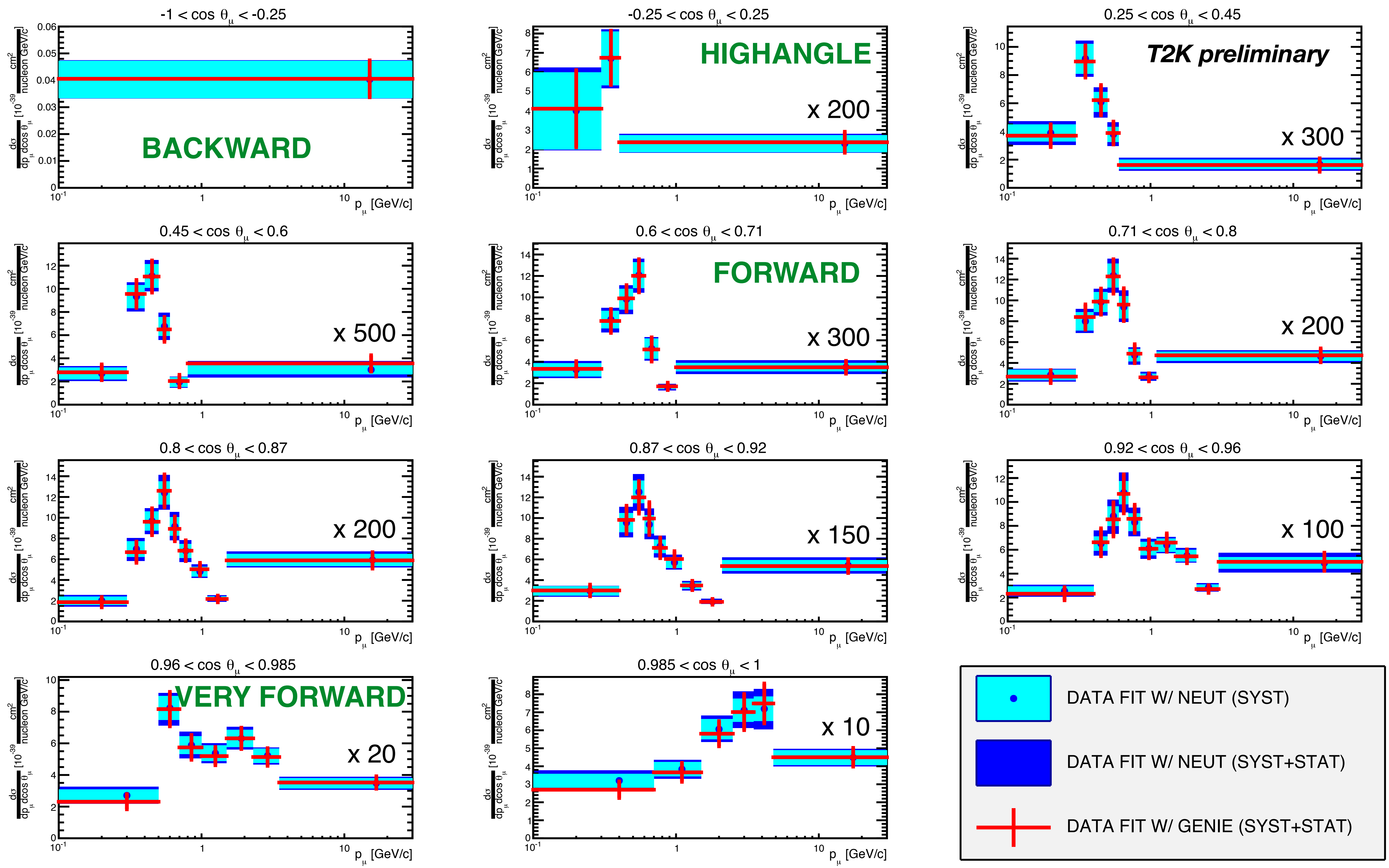

-1 < cos θμ < -0.25
BACKWARD
-0.25 < cos θμ < 0.25
HIGHANGLE
x 200
0.25 < cos θμ < 0.45
T2K preliminary
x 300
0.45 < cos θμ < 0.6
x 500
0.6 < cos θμ < 0.71
FORWARD
x 300
0.71 < cos θμ < 0.8
x 200
0.8 < cos θμ < 0.87
x 200
0.87 < cos θμ < 0.92
x 150
0.92 < cos θμ < 0.96
x 100
0.96 < cos θμ < 0.985
VERY FORWARD
x 20
0.985 < cos θμ < 1
x 10
pμ [GeV/c]
DATA FIT W/ NEUT (SYST)
DATA FIT W/ NEUT (SYST+STAT)
DATA FIT W/ GENIE (SYST+STAT)

NEW Results:

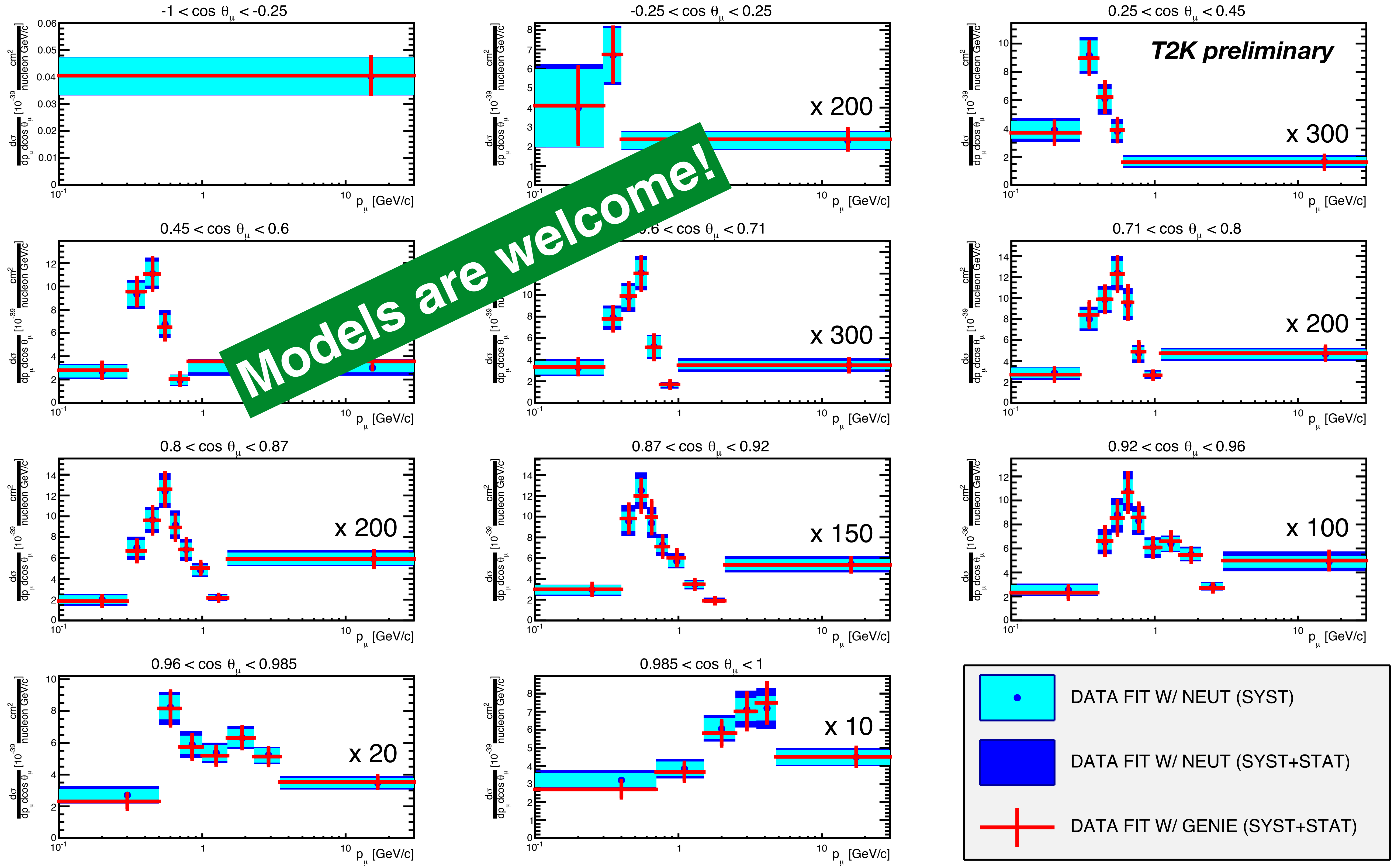
-1 < cos θμ < -0.25
-0.25 < cos θμ < 0.25
x 200
0.25 < cos θμ < 0.45
T2K preliminary
x 300
0.45 < cos θμ < 0.6
0.6 < cos θμ < 0.71
x 300
0.71 < cos θμ < 0.8
x 200
0.8 < cos θμ < 0.87
x 200
0.87 < cos θμ < 0.92
x 150
0.92 < cos θμ < 0.96
x 100
0.96 < cos θμ < 0.985
x 20
0.985 < cos θμ < 1
x 10
pμ [GeV/c]
Models are welcome!
DATA FIT W/ NEUT (SYST)
DATA FIT W/ NEUT (SYST+STAT)
DATA FIT W/ GENIE (SYST+STAT)

Conclusions:

- T2K near detectors provide a perfect opportunity to make precise cross section measurements.
- ν_μ CC selection has been improved in order to increase both purity and angular acceptance.
- New inclusive cross-section measurement has been developed using new selection.
- Other on-going inclusive analyses:
  - $\sigma_{water}/\sigma_{scint}$ using two FGDs sub-detectors in ND280 (off-axis).
  - ν_μ CC-inclusive cross section with H_2O using INGRID (on-axis).
  - Run 8 will increase by a factor ~2 statistics.

Back up

Off-axis Neutrino Flux:

- Off-axis neutrino flux -> narrow peak centred at ~600 MeV.
- Low multiplicity interactions are dominant in this energy region.
- Nuclear medium plays a fundamental role.

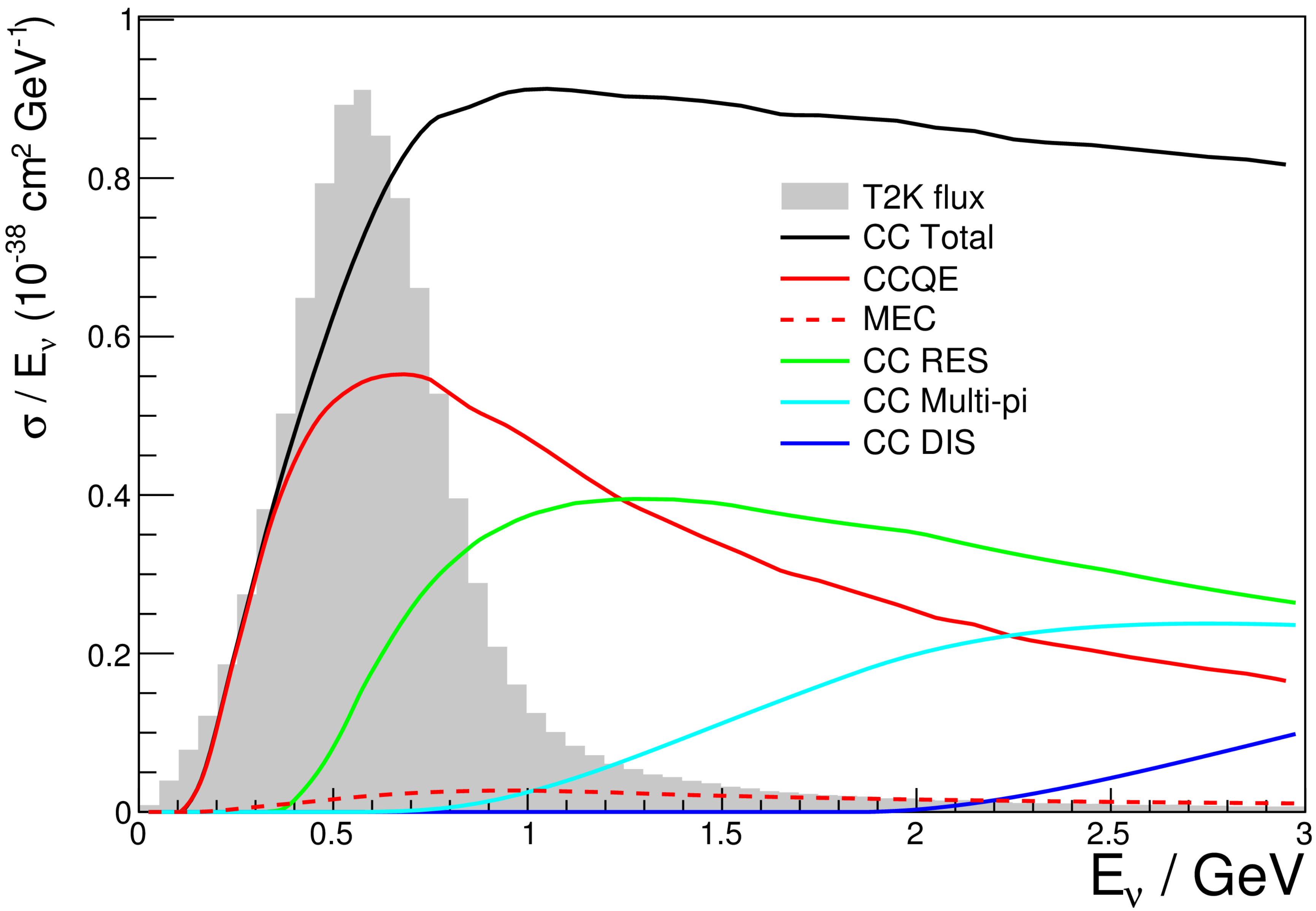

Event generators:

	NEUT 5.3.2	GENIE 2.8.0
CCQE	SF (Benhar et al., 2000) BBA05 (Bradford et al., 2005) M_A^{QE} = 1.21 GeV/c^2 p_F [^{12}C] = 217 MeV/c E_B [^{12}C] = 25 MeV	RFG (Bodek et al., 1981) BBA05 (Bradford et al., 2005) M_A^{QE} = 0.99 GeV/c^2 p_F [^{12}C] = 221 MeV/c E_B [^{12}C] = 25 MeV
2p2h	Nieves et al., 2011	-
CCRES	W<2 GeV Rein-Sehgal, 1981 FF (Graczyk et al., 2008)	W<1.7 GeV Rein-Sehgal, 1981 FF (Kuzmin et al., 2016)
CCDIS	W>1.3 GeV (w/o single π) GRV98 PDF (Glück et al. 1998) BY corr. at low Q2 (Bodek et al. 2003)	W>1.7 GeV (for W<1.7 GeV is tuned) GRV98 PDF (Glück et al. 1998) BY corr. at low Q2 (Bodek et al. 2005)
Hadronization	W < 2 GeV KNO scaling (Koba et al. 1972) W > 2 GeV PYTHIA/JETSET	W < 2.3 GeV AGKY (Koba et al. 1972) 2.3 GeV < W < 3 GeV AGKY (Koba et al. 1972) + PYTHIA/JETSET W > 3 GeV PYTHIA/JETSET
FSI	Intra-nuclear cascade	Intra-nuclear cascade (INTRANUKE hA)

Momentum distribution:

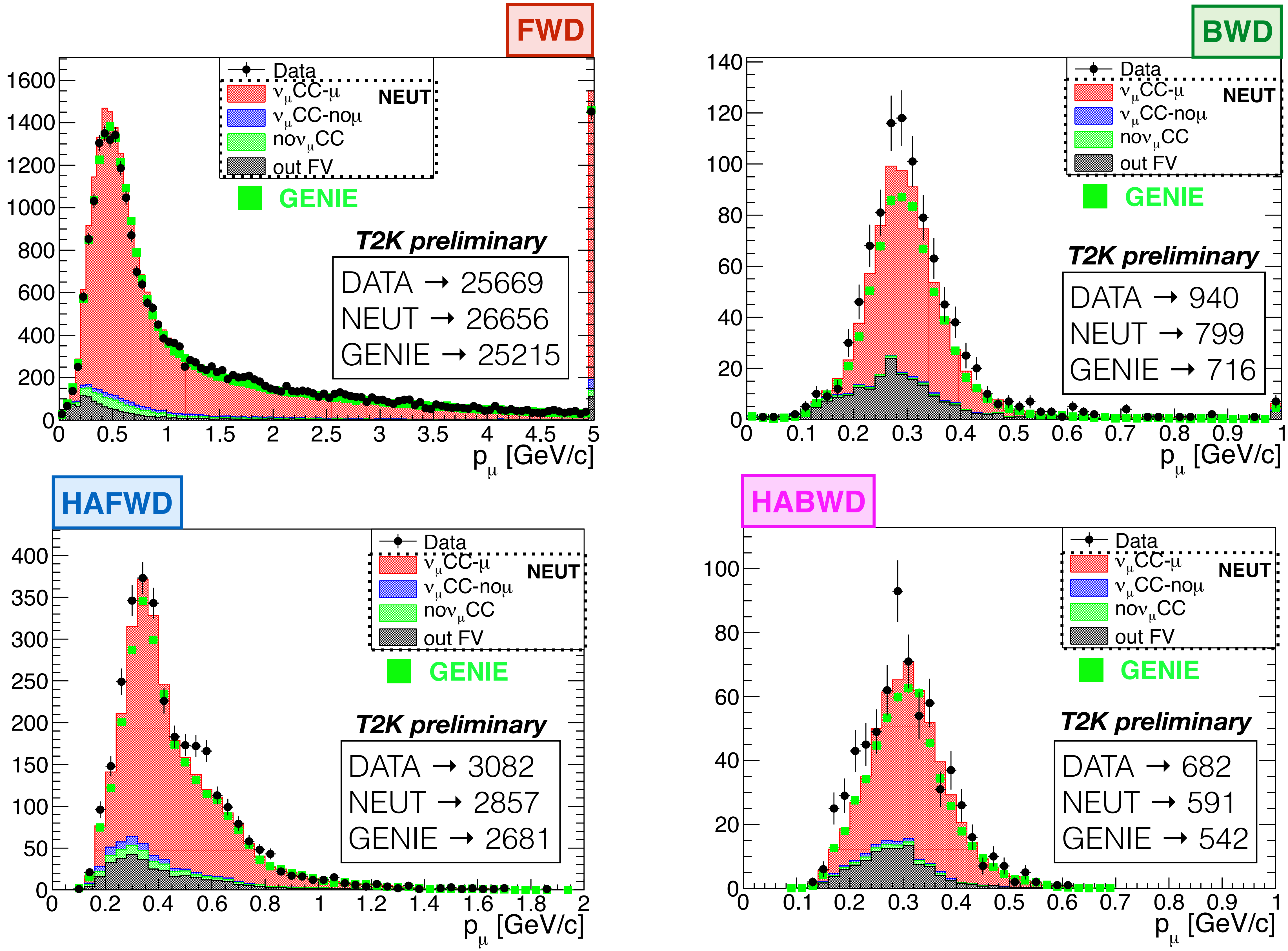

Angular distribution:

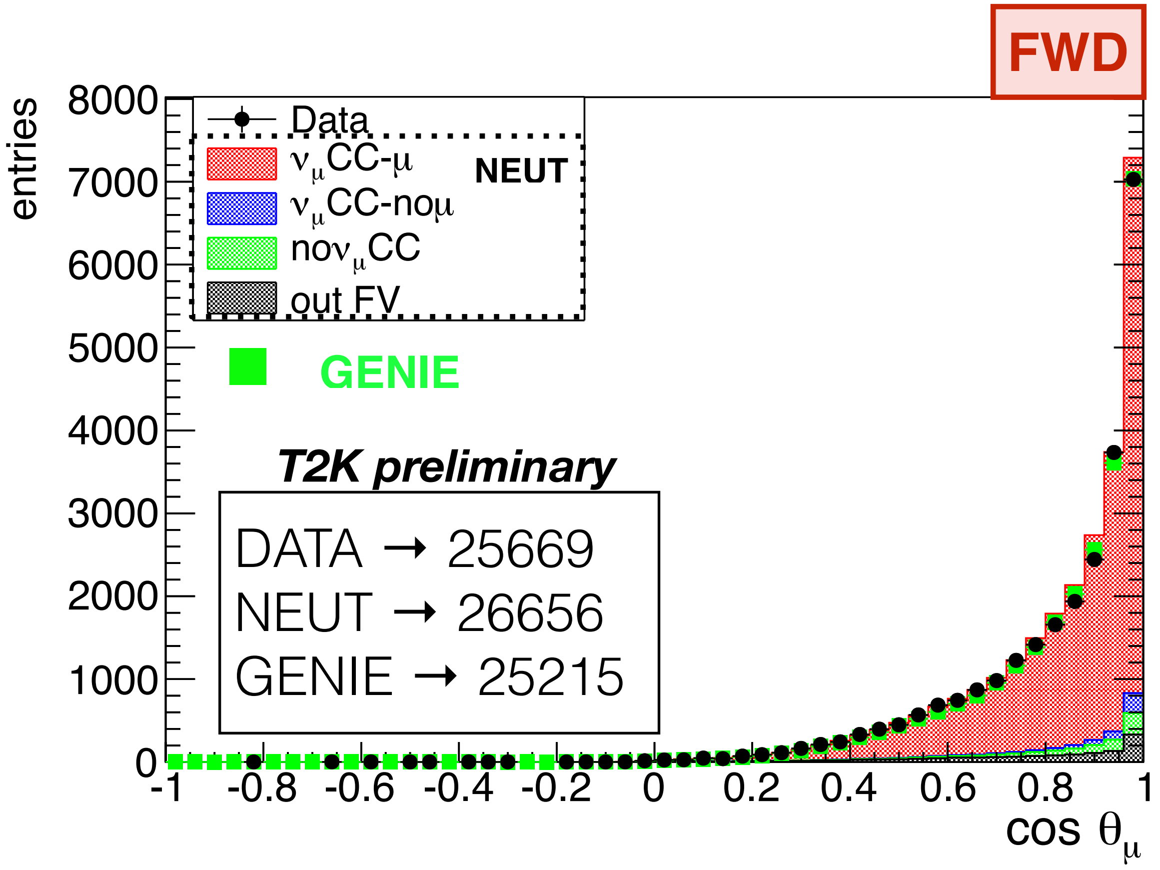

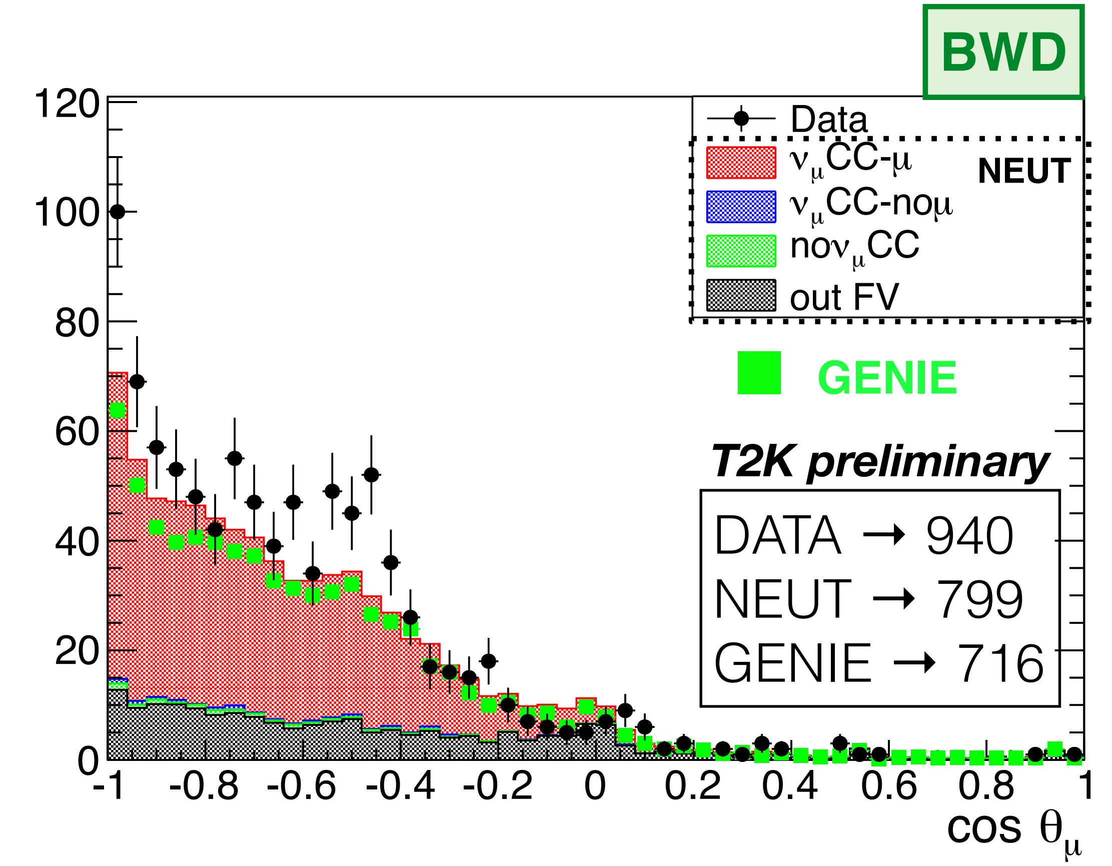

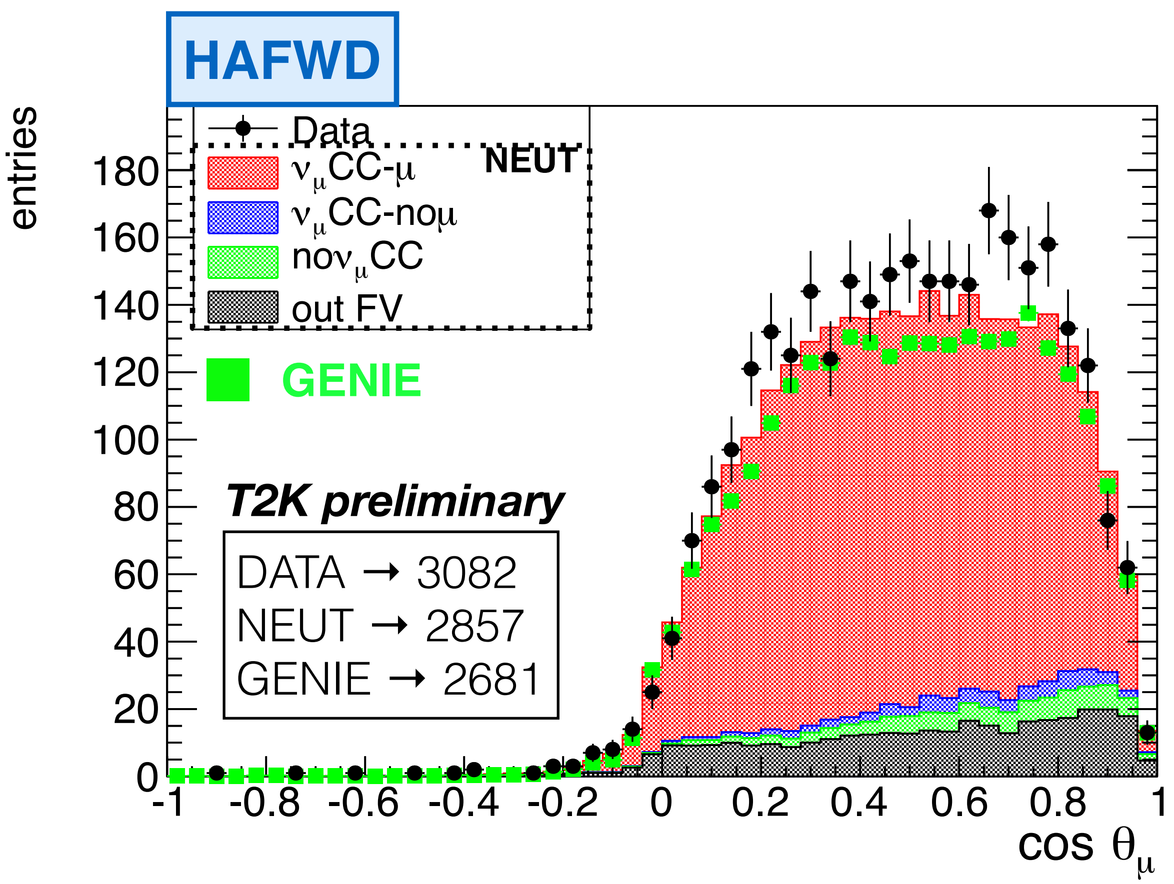

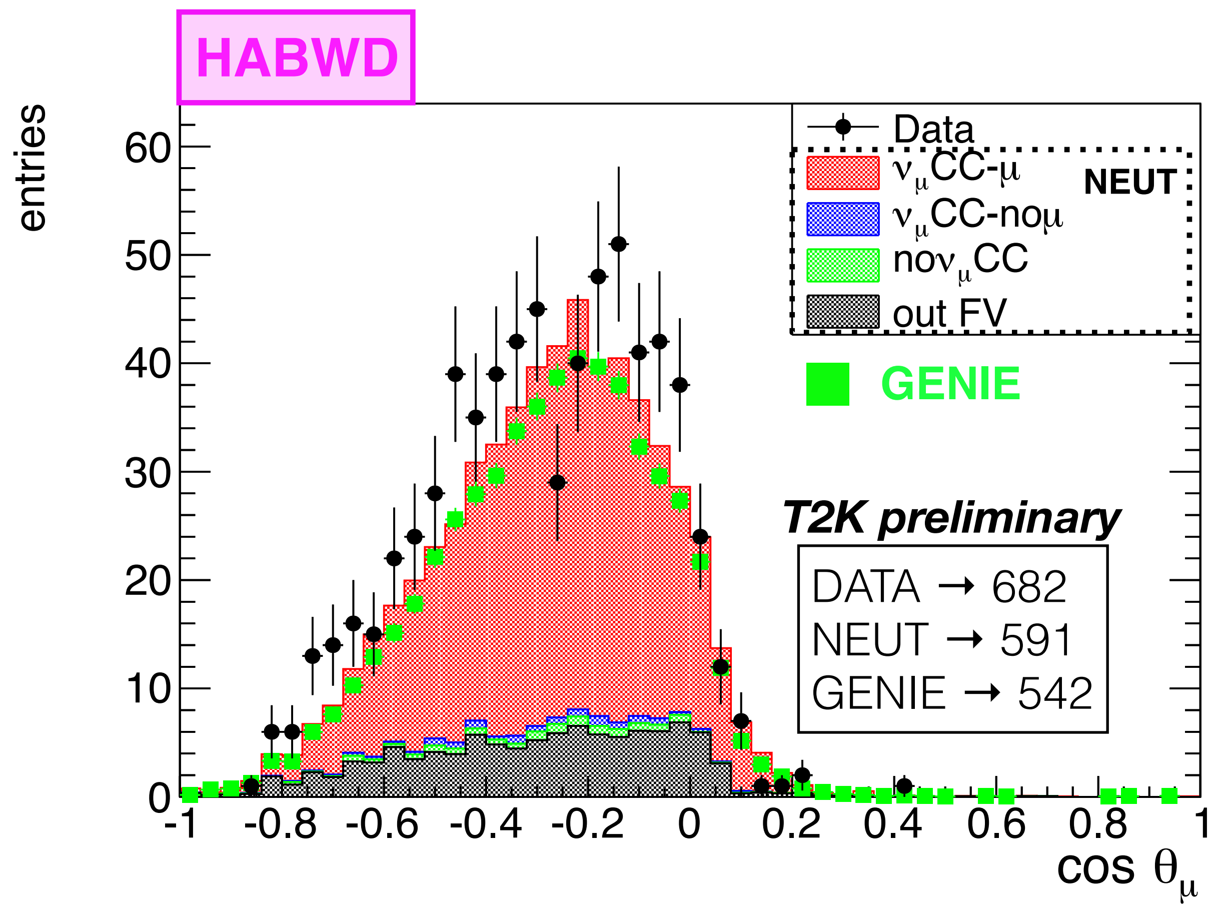

Sidebands:

- Try to constrain π^- background modelling (NC and pion FSI).

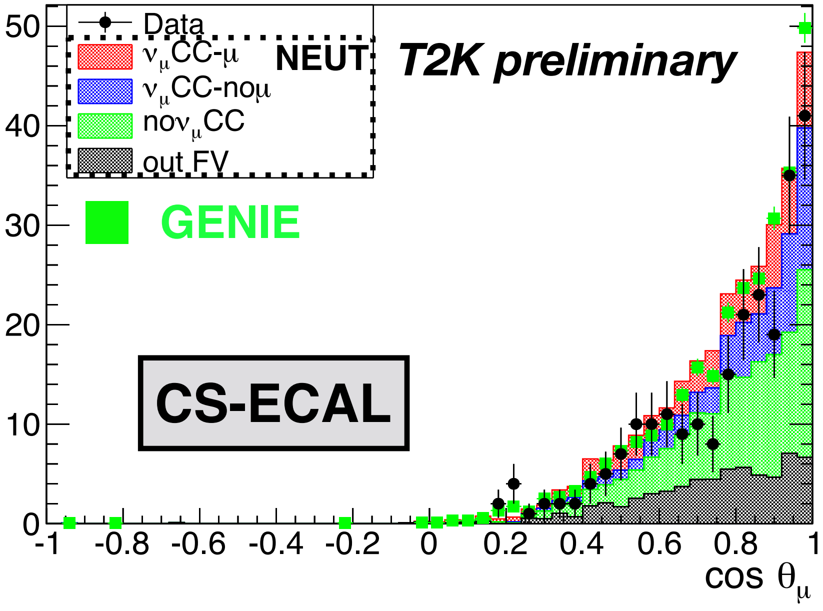

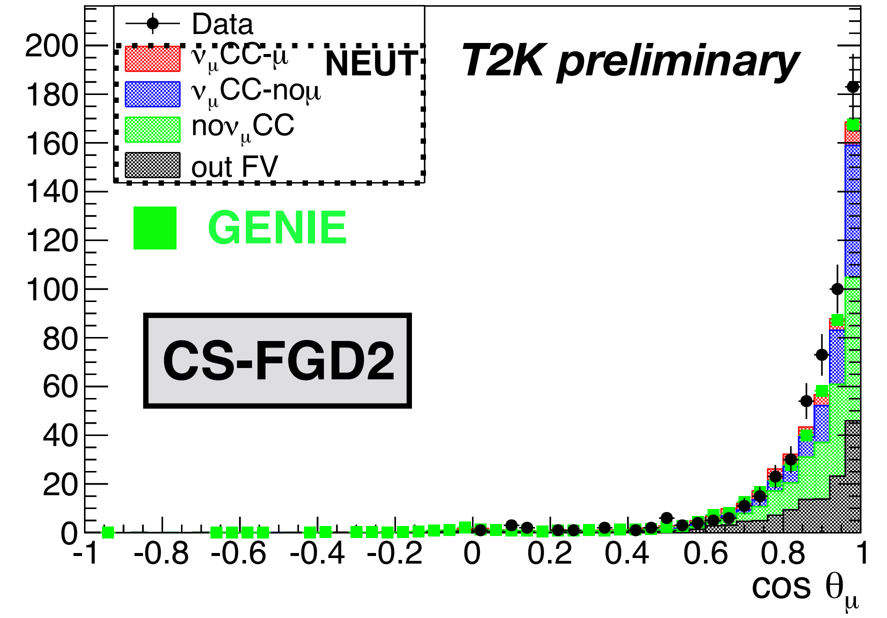

- Highly pure π^- sample.
- Sidebands and background in signal selection have similar shape.

π^- BCKG → NEUT & GENIE = ~1500 events(~6%)

π^- SIDEBANDS → NEUT & GENIE = ~750 events (~70%)

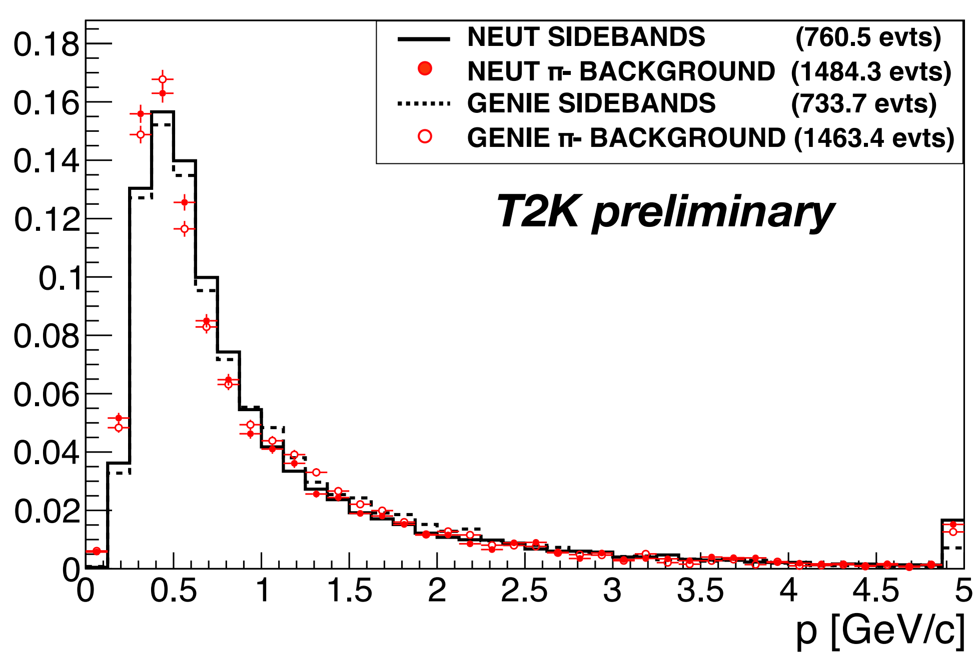

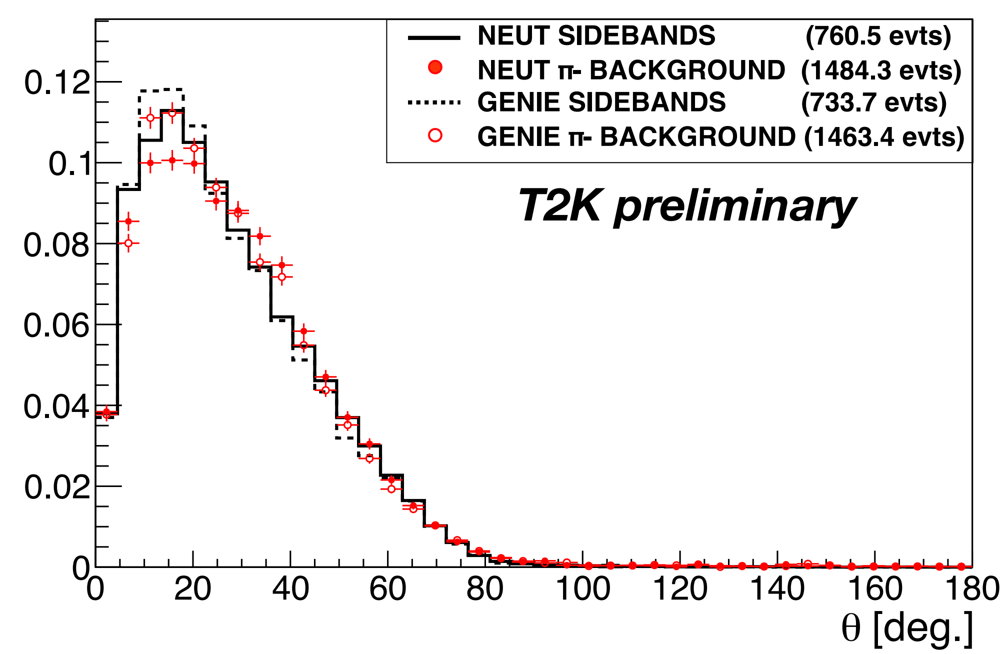

Efficiency:

- Efficiency computed with two different MC:

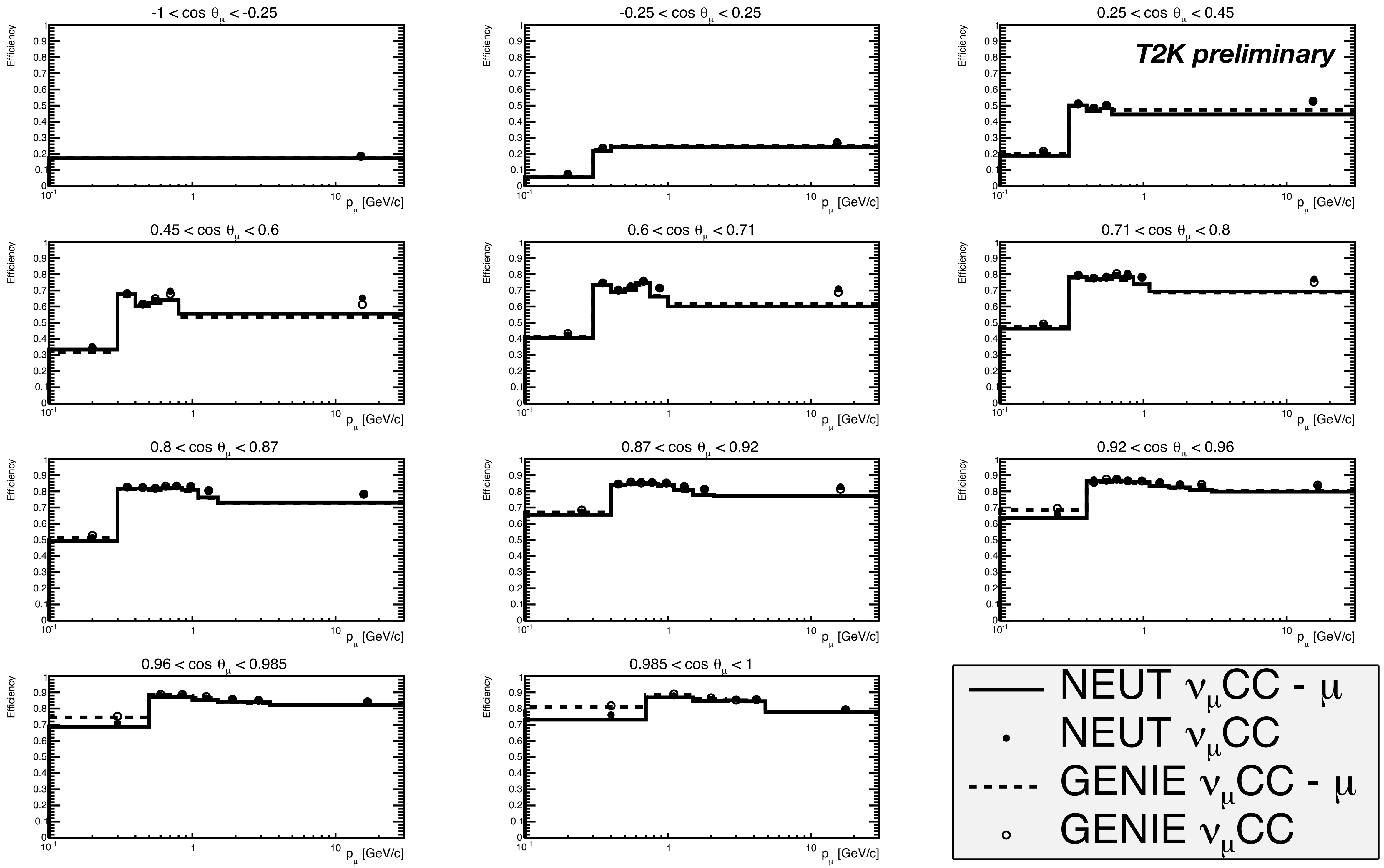

Systematics uncertainties:

$$\frac{d\sigma}{dp_{\mu,i}dcos\theta_{\mu,j}} = \frac{N_{ij}^{CC-\mu}}{\epsilon_{ij}^{CC-\mu,MC}\Phi N_{nucleons}^{FV}\Delta p_{\mu,i}\Delta cos\theta_{\mu,j}}$$

MODELLING

π FSI

Dial	Code	Type	Prior	Error	Valid range
FSI_INEL_LO_E	kNCasc_FrInelLow_pi	Shape	0.0	0.41	[−0.8, 1.2]
FSI_INEL_HI_E	kNCasc_FrInelHigh_pi	Shape	0.0	0.34	[−0.8, 1.2]
FSI_PI_PROD	kNCasc_FrPiProd_pi	Shape	0.0	0.5	[−0.8, 1.2]
FSI_PI_ABS	kNCasc_FrAbs_pi	Shape	0.0	0.41	[−0.6, 0.9]
FSI_CEX_LO_E	kNCasc_FrCExLow_pi	Shape	0.0	0.57	[−0.8, 1.2]
FSI_CEX_HI_E	kNCasc_FrCExHigh_pi	Shape	0.0	0.28	[−0.8, 1.2]

NUISANCE

π HADRON

Dial	Code	Type	Prior	Error	Valid range
AGKY_xF1pi	kGHadrAGKY_xF1pi	Shape	0	0.2	[−9999, 9999]
AGKY_pT1pi	kGHadrAGKY_pT1pi	Shape	0	0.03	[−9999, 9999]
Nucl_FormZone	kGHadrNucl_FormZone	Shape	0	0.5	[−9999, 9999]
Theta_Delta2Npi	kGRDcy_Theta_Delta2Npi	Shape	0	1	[−1, 1]

XSEC

Dial	Code	Type	Prior	Error	Valid range
MAQE	kNXSec_MaCCQE	Shape	1.2	0.3	[0, 9999]
pF_C	kNIWG2014a_pF_C12	Shape	217	30	[200, 275]
MEC_C	kNIWGMEC_Norm_C12	Norm	1	1	[0, 9999]
EB_C	kNIWG2014a_Eb_C12	Shape	25	30	[12, 42]
pF_O	kNIWG2014a_pF_O16	Shape	225	30	[200, 275]
MEC_O	kNIWGMEC_Norm_O16	Norm	1	1	[0, 9999]
EB_O	kNIWG2014a_Eb_O16	Shape	27	30	[12, 42]
CA5	kNXSec_CA5RES	Shape	1.01	0.12	[0, 9999]
MANFFRES	kNXSec_MaNFFRES	Shape	0.95	0.15	[0, 9999]
BgRES	kNXSec_BgSclRES	Shape	1.3	0.2	[0, 9999]
DISMPISHP	kNIWG2012a_dismpishp	Shape	0	0.4	[−9999, 9999]
CCCOH_C_0	kNIWG2012a_cccohE0	Norm	1	0.3	[0, 9999]
CCCOH_O_0	kNIWG2012a_cccohE0	Norm	1	0.3	[0, 9999]
CNUE_0	kNIWG2012a_ccnueE0	Norm	1	0.03	[0, 9999]
CNUEBAR_0	kNIWG2012a_ccnueE0	Norm	1	0.03	[0, 9999]
NCCOH_0	kNIWG2012a_nccohE0	Norm	1	0.3	[0, 9999]
NCOTHER_0	kNIWG2012a_ncotherE0	Norm	1	0.3	[0, 9999]

NUISANCE

Total uncertainties:

- Flux+DataSTAT dominates with low modelling uncertainties (except backward region).

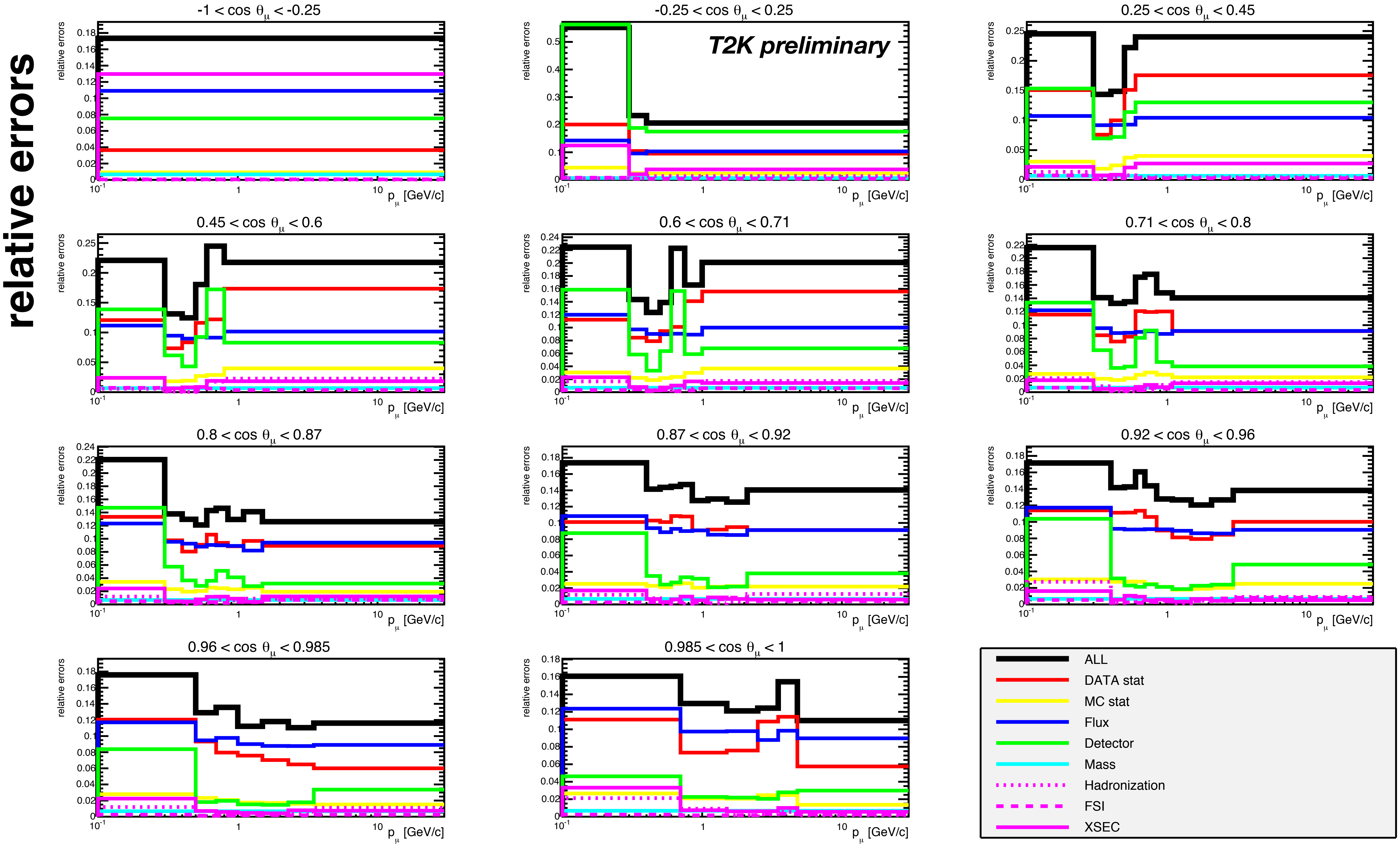

Integrated cross section result:

- Integrated result matches previous analysis.
- Error reduced from 12% to 9% (flux dominates).

<E_ν> = 0.85 GeV
[2014] ~1.1x10^{20}POT
σ = 0.698+-0.085 $cm^2 nucleon^{-1}$
[2017] ~5.8x10^{20}POT
σ = 0.700+-0.064 $cm^2 nucleon^{-1}$

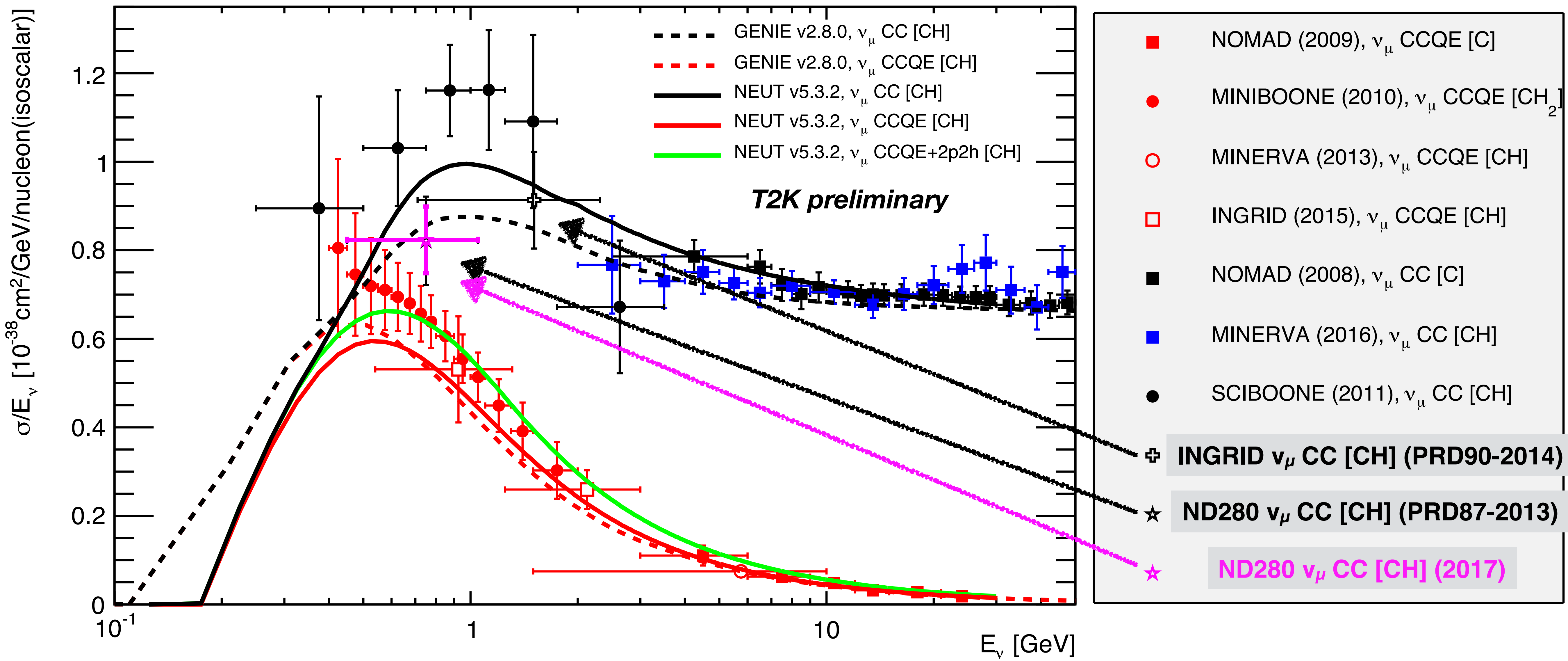

Real data results:

- Consistent with previous measurement.

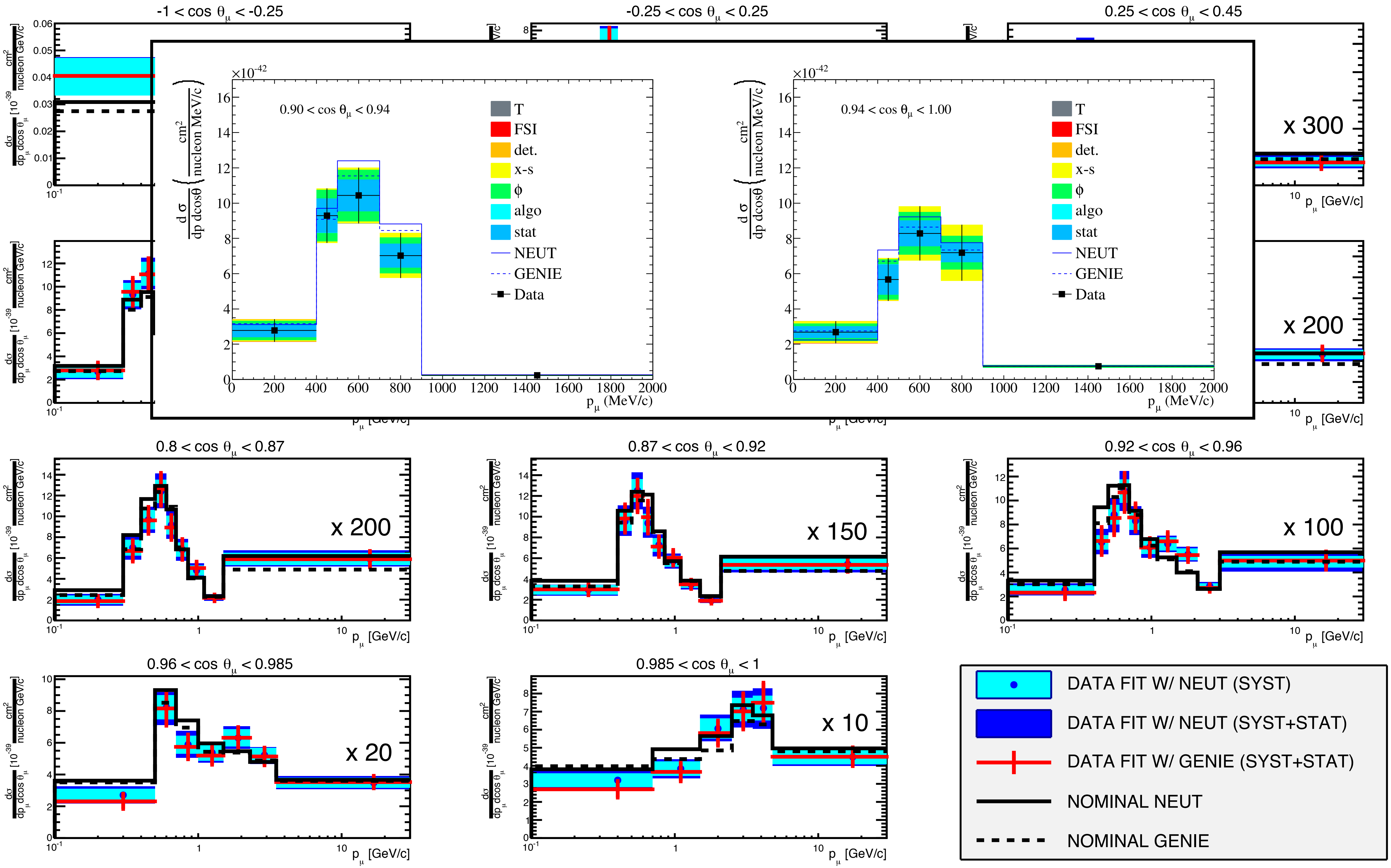

Models comparison:

- Versions:
    - NEUT 5.3.2
    - GENIE 2.8.0
    - NuWro 11

	NEUT-SF	NEUT-RFG	NEUT-RFG+RPA	NEUT-NIWG	GENIE	NUWRO
Nuclear model	SF	RFG	RFG	RFG	RFG	LFG
M_A^{QE} [GeV/c^2]	1.21	1.21	1.21	1.15	0.99	1.2
p_F [MeV/c]	217	217	217	223	221	-
E_B [MeV]	25	25	25	25	25	25
MEC-Nieves %	100	100	100	27	0	100
RPA	No	No	Yes	Yes	No	No
DATA fit w/ NEUT						
χ^2 (χ^2_{SHAPE})	211.9 (210.1)	284.8 (242.6)	173.4 (168.1)	160.9 (179.4)	191.3 (232.2)	471.4 (457.9)
DATA fit w/ GENIE						
χ^2 (χ^2_{SHAPE})	227.4 (221.8)	300.6 (253.4)	192.6 (182.9)	175.3 (191.2)	190.5 (224.4)	465.7 (458.5)

NBINS = 71

Models comparison:

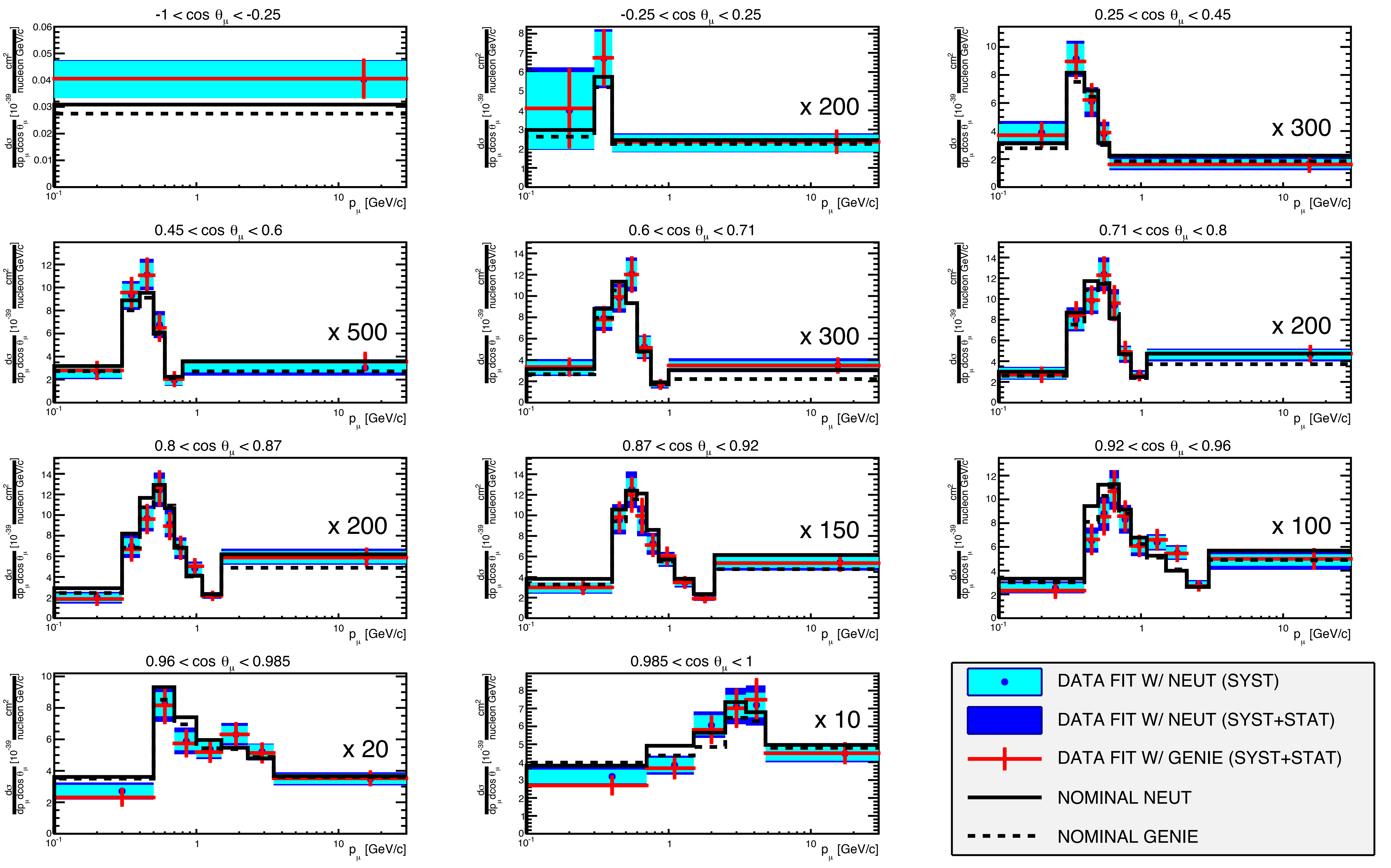

Models comparison:

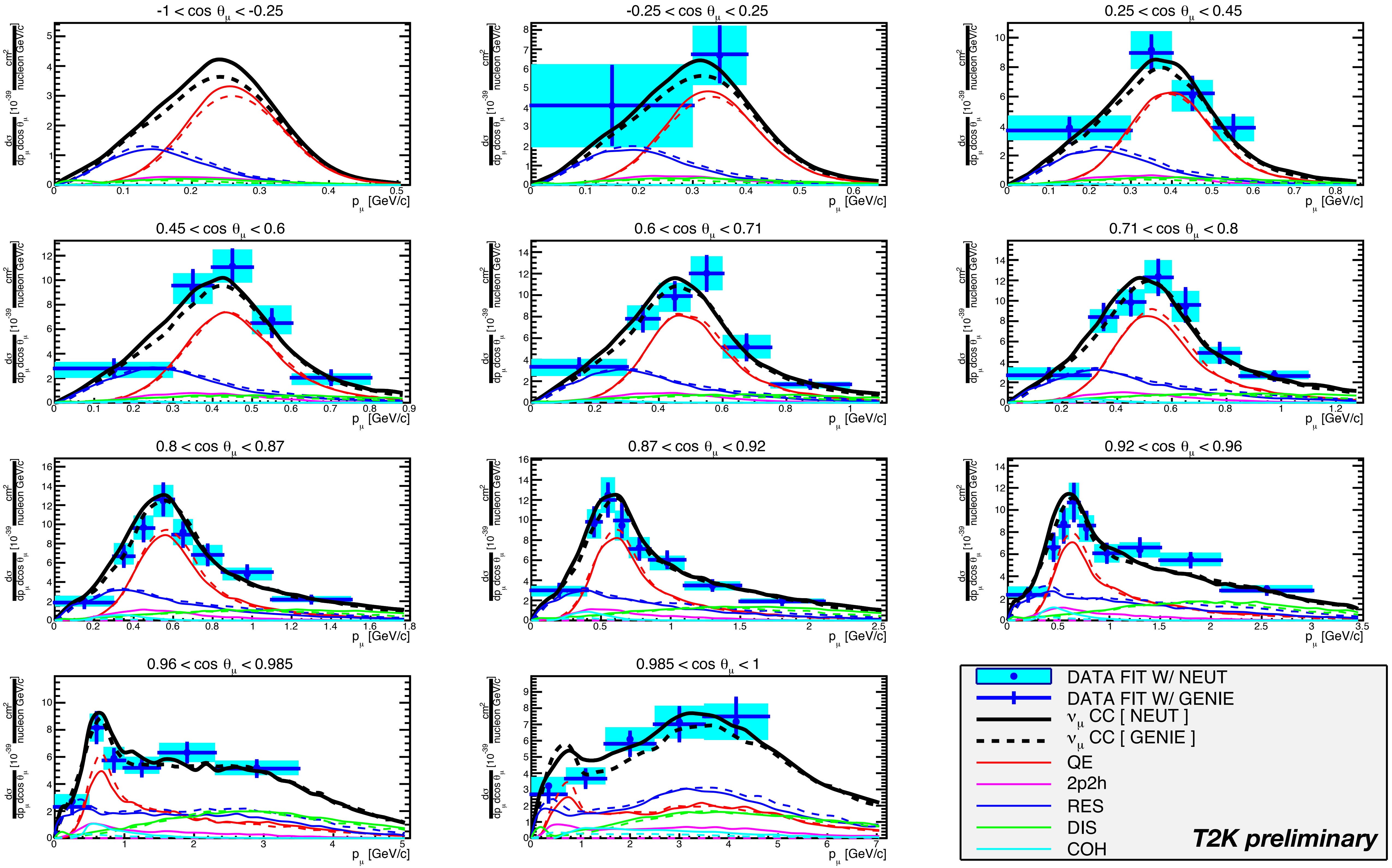

Models comparison:

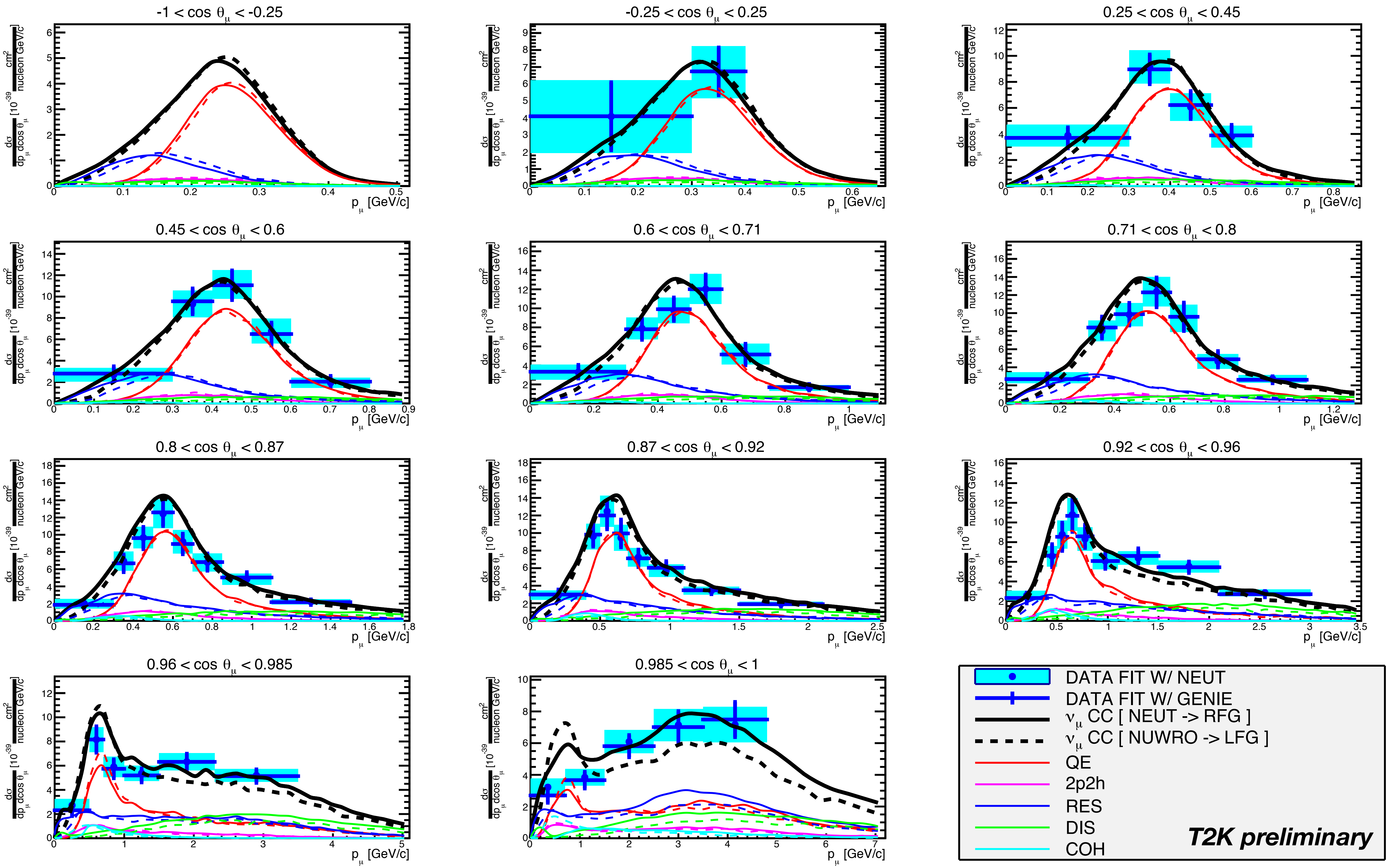

Real data result: